Characterizing Quark Gluon Plasma through particle ratio

Rutik Poozhikkunnath
Roll No: MS15086

A dissertation submitted for the partial fulfilment
of BS-MS dual degree in Science

Under the guidence of
Dr. Satyajit Jena

June 2020

Indian Institute of Science Education and Research Mohali
Sector - 81, SAS Nagar, Mohali 140306, Punjab, India

Certificate of Examination

This is to certify that the dissertation titled **"Characterizing Quark Gluon Plasma through particle ratio"** submitted by **Rutik Poozhikkunnath** (Reg. No. MS15086) for the partial fulfillment of BS-MS dual degree programme of the Institute, has been examined by the thesis committee duly appointed by the Institute. The committee finds the work done by the candidate satisfactory and recommends that the report be accepted.

Dr. Ambresh Sivaji Dr. Anosh Joseph Dr. Satyajit Jena
(Supervisor)

Dated: 15.06.2020

Declaration

The work presented in this dissertation has been carried out by me under the guidance of Dr. Satyajit Jena at the Indian Institute of Science Education and Research Mohali.

This work has not been submitted in part or in full for a degree, a diploma, or a fellowship to any other university or institute. Whenever contributions of others are involved, every effort is made to indicate this clearly, with due acknowledgement of collaborative research and discussions. This thesis is a bonafide record of original work done by me and all sources listed within have been detailed in the bibliography.

Rutik Poozhikkunnath
(Candidate)

Dated: June 15, 2020

In my capacity as the supervisor of the candidate's project work, I certify that the above statements by the candidate are true to the best of my knowledge.

Dr. Satyajit Jena
(Supervisor)

Acknowledgement

First and foremost, I would like to thank my thesis supervisor Dr. Satyajit Jena, without whose help and supervision, this thesis would have never been possible. The discussions that I had with him has enhanced my capabilities as a researcher.

I would also like to thank my thesis committee members Dr. Anosh Joseph and Dr. Ambresh Shivaji for their valuable suggestions and criticism of my work.
I owe my deepest gratitude to Rohit Gupta for helping me with the discussions and in learning the basics of the ROOT Framework. I would like to mention my heartiest gratitude to all my lab members.
I would like to thank all my friends for supporting and helping me during the entire period of the project. I would like to acknowledge the moral support and encouragement, that I have received from my parents and brother.
I would also like to acknowledge DST INSPIRE, Government of India for the financial support.

Rutik Manikandhan
MS15086
IISER Mohali.

List of Figures

Contents

Abstract

According to Big-Bang theory, at the earliest of its expansion, universe existed as QGP. As it cooled down, the deconfinement-confinement phase transition occurred and hadrons were formed. Study about this kind of a stage can lead us to understand the early stages of universe formation. It can also give us some constraints on the Standard Model which can give us insights to the formation of theories beyond the Standard Model. The transformation of matter at high enough energies, from nucleons to constituent quarks and gluons has been very interesting and equally very challenging.

Even though the energy scale is quite challenging, in heavy ion collisions we are trying to create a similar system and studying various properties. Since the multiplicity of produced particles is an important quantity to characterise the evolving system and its event to event fluctuation may provide a distinct signal of the phase transition from hadron gas to QGP. This signal is to be found using ν Dynamics. Higher moments of a distribution can give important information about the asymmetry of the system. Considering the distributions of conserved quantities in this system, higher moment analysis provide a scope to understand some existing problems. In this thesis we are looking at the higher moments of such multiplicity distributions and ν Dynamics analysis to reveal some dynamical fluctuations. Study of higher moments like kurtosis and skewness of these multiplicity distributions on an event-by-event basis will provide valuable information on the dynamic state of the system just after the collision. From these higher moments we can also calculate the susceptibilities of the system which is very useful in determining whether there are any fluctuations due to QGP formation or it's the Hadron Phase fluctuations. These studies are geometrical studies i.e they are characterised using centrality or number of participating nucleons ($\langle N_{part} \rangle$). Charged particle multiplicity distributions are studied for Pb-Pb collisions at $\sqrt{S_{NN}}$ = 2.76 TeV.

Chapter 1

Introduction

1.1 Standard Model

Presently the answer we have to the widely asked question, what the world is made up of is the Standard Model, the reason behind the 2013 Nobel Prize. At the same time the 2015 Nobel Prize renders this theory incomplete and hence this new search for Beyond the Standard Model.

The Standard Model classifies the whole universe into elementary particles called the Leptons and Hadrons as shown in Figure 1.1. The theoretical basis that we were taught in our schools where the atoms is the smallest unit which comprises of protons, neutrons and electrons were rendered incomplete when inelastic electron-proton scattering experiments were performed which showed that protons have a substructure comprising of particles called quarks. Further experiments showed that neutrons too have a substructure comprising of quarks.

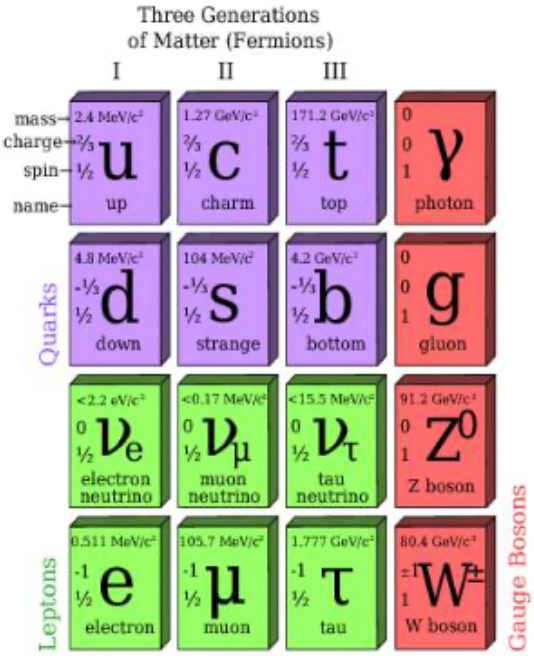

Figure 1.1: Three generation of matter particles in the standard model. The mediator particles (Gauge bosons) are also shown. [Cha14]

Proton contains two up and one down quark whereas a neutron contains two down and one up quark. The quarks interact with each other via the exchange of gluons. The force existing between the quarks is called the **color force**. Quarks and gluons are collectively known as **partons** (the *parton* name was given by Feynman, while Murray Gellman picked the word *quark* from the sentence Three quarks for Muster Mark in James Joyce book, Finnegans Wake). This color force which is the backbone of the Quantum Chromo Dynamics (QCD) is what describes one of the fundamental forces called the strong interaction force shown in Table 1.2.

Quarks come in six flavors: u (up), d (down), s (strange), c (charm), t (top), b (bottom) and each quark may exist in three equivalent states differing in values of the new quantum number, termed as color.

1.2 Color the Quantum Number

Pauli exclusion principle forbids two identical fermions to occupy same quantum state. However, making up hadrons from quarks, possessing spin 1/2, will lead to a contradiction to the exclusion principle, for example, proton contains two up quarks and Ω^- particle is made of three strange quarks. The existence of such particles indicate that there must exist some another quantum number (in addition to spin) and since a maximum of three quark bound states exist in nature (baryons), this new quantum number must have three values. In 1965 three physicists Bogolubov, Struminsky, Tavkhelidze introduced the concept of color quantum number with colored quarks existing in three states, red (R), green (G) and blue (B).

Since quarks are charged, they will also interact by photon exchange i.e. via electromagnetic interactions. Considering the existence of Δ++ particle, containing three u quarks, there must exist a **strong** force that will overrule the electromagnetic repulsion between u quarks and bind these quarks together to form Δ++ particle. In fact, a color charge endows the quarks with a new color field making this strong binding possible. As indicated earlier, gluons are the quanta of this color field.

Gluon itself is a colored object, in fact its a bicolored object (color + anticolor). Since there are three color states; R, G, B and correspondingly three anticolor states; antired($\overline{R}$), antigreen ($\overline{G}$), antiblue ($\overline{B}$) which on permuting we can have nine bicolored states: $R\overline{R}$, $R\overline{G}$, $R\overline{B}$, $G\overline{R}$, $G\overline{G}$, $G\overline{B}$, $B\overline{R}$, $B\overline{G}$, $B\overline{B}$. One of the nine combinations $R\overline{R}$ + $G\overline{G}$ + $B\overline{B}$ is a color singlet state which lacks any net color charge and thus cannot play the role of a gluon carrying color from one quark to another.

Quantum Chromodynamics (QCD) is the theory of strong interactions between quarks and gluons. It is a theory like electromagnetism but with eight gluons instead of a single photon. There is other important distinctions between the two theories:

- Photons are neutral particles, they do not carry any electric charge but gluons are colored objects.

- The coulomb interactions between electric charges vary inversely as the distance between the charges whereas, as pointed out earlier, the color force strength increases with the distance between quarks.

1.3 Asymptotic Freedom

The color force between the quarks tend to be weak when quarks are close together. Within a proton (or other hadron), at distances of less than 1 fermi, quarks behave as if they were nearly free. However, when one begins to draw the quarks apart, the force grows stronger. This is because gluons have the ability to create other gluons. Thus, if a quark starts to speed away from another quark after being struck by an accelerated particle, the gluons utilize this energy to produce more gluons. More the number of gluons exchanged among quarks, stronger will be the color force. At some point the force will grow so strong that an additional quark-antiquark pair production energy will be reached before the quarks can be separated. This is why quarks cannot be isolated and this is known as color confinement. This behaviour of color force is taken into account in the QCD theory by defining a *running* coupling constant.

1.4 Why the QGP ?

For a few millionths of a second after the Big-Bang, the universe was filled with an extremely hot and dense soup of quarks and gluons known as the quark-gluon-plasma (QGP) [Alf03]. Also known as the primordial fluid (detailed study of the QGP shows it has lowest shear viscosity to entropy ratio making it the most perfect fluid in the universe Table 1.3). The existence of this novel phase of matter was proposed in the mid-seventies, just ten years after the birth of the Quark Model of hadrons, and two years after it was realised that the

candidate non-Abelian field theory of inter-quark forces, which is quantum chromodynamics (QCD) predicts their weakening at short distances, the so-called asymptotic freedom. As the universe cooled down, the quarks and gluons hadronize resulting in the formation of baryonic matter that we see today.

Fluid	p [Pa]	T [K]	η [Pa·s]	η/n [$\hbar$]	η/s [$\hbar/k_B$]
H_2O	0.1×10^6	370	2.9×10^{-4}	85	8.2
^{4}He	0.1×10^6	2.0	1.2×10^{-6}	0.5	1.9
H_2O	22.6×10^6	650	6.0×10^{-5}	32	2.0
^{4}He	0.22×10^6	5.1	1.7×10^{-6}	1.7	0.7
^{6}Li ($a=\infty$)	12×10^{-9}	23×10^{-6}	$\leq1.7\times10^{-15}$	≤1	≤0.5
QGP	88×10^{33}	2×10^{12}	$\leq5\times10^{11}$		≤0.4

Figure 1.2: The viscosity η,the viscosity over density η/n ratio, and the viscosity over entropy density η/s ratio for several fluids at particular values of pressure p and temperature T (from Ref. [ST09])

1.5 Formation of the QGP

At high densities once we have a system of interpenetrating hadrons, each quark will find in its vicinity, at a distance less than the hadron radius, a number of quarks. In this state each quark's identity is lost now and neighbouring quarks have no meaning. We say now the quarks are in a deconfined state.

This state can also be achieved by increasing the temperature and at high enough temperatures more and more low mass pions will be formed and thereby increasing the density.

This kind of transition from a confined state to a deconfined state is very similar to phase transitions we see in thermodynamic systems but here the derivatives of free energy do not posses any singularity at the transition point hence not so trivial. But still can be probed using order parameters and other state variables.

Now the deconfined state of quarks are bag of particles, a macroscopic system which can be characterized with state variables.

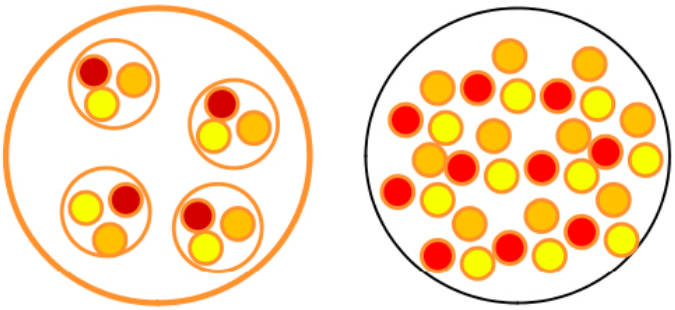

Figure 1.3: The figure on the left shows a nucleus at low energy density / temperature and the figure on the right shows the same system at extreme conditions of energy density / temperature

1.5.1 Mechanism of the Mott Transition

The mechanism of deconfinement is provided by the screening of the color charge. It is analogous to the Mott transition in atomic physics. In dense matter, the long range coulomb potential, which binds ions and electrons into electrically neutral atom, is partially screened due to presence of other charges, the potential become much more short range,

$$V(r) = e_0^2/r \ \rightarrow \ e_0^2/r \times exp(-r/r_D) \tag{1.1}$$

here r is the distance of the probe from the test charge e_0. r_D is the Debye screening radius and is inversely proportional to density,

$$r_D \sim n^{-1/3} \tag{1.2}$$

At sufficiently high density, r_D can be smaller than the atomic radius. A given electron can no longer feel the binding force of its ion, alternatively, at such density, coulomb potential can no longer bind electron and ion into a neutral atom. The insulating matter becomes a conducting matter. This is the Mott transition. We expect deconfinement to be the quantum chromodynamic analog of Mott transition.

Due to the screening of color potential, quarks can not be bound into a hadron. Now one may wonder about the very different nature of QCD and QED forces. Interaction potential in QED and QCD can be expressed as,

$$QED : V(r) \sim e^2/r \tag{1.3}$$

$$QCD : V(r) \sim \text{-}\alpha/r + \sigma r \tag{1.4}$$

While in QED, potential decreases continuously with increasing distance, in QCD, at large distance, it increases with distance. However, screening is a phenomenon at high density, or at short distance. The difference in QED and QCD at large distance is of no consequence then. More over, due to asymptotic freedom, in QCD interaction strength decreases at short distances, thereby enhancing the deconfinement.

1.6 Stages of Heavy-Ion collisions

The Large Hadron Collider (LHC) at CERN and Relativistic Heavy-Ion Collider (RHIC) at BrookHaven National Laboratory (BNL) make head-on collisions between massive ions at very high energies to recreate conditions similar to those of the very early universe.
Such a relativistic nucleus-nucleus collision passes through different stages which are described below:

- **Pre-equilibrium Stage:** Initial partonic collisions produce a fireball in a highly excited state. In all possibility, the fireball is not in equilibrium. Constituents of the system collide frequently to establish a local equilibrium state. The time takes to establish local equilibrium is called thermalisation time T. The state of matter for 0 $<$ t $<$ T is said to be in the pre-equilibrium stage.

- **Expansion stage and Hadronization:** In the equilibrium or the thermalised state, the system has thermal pressure which acts against the surrounding vacuum. The system then undergoes collective (hydrodynamic) expansion. As the system expands, its density (energy density) decreases and the system cools. The expansion and cooling is governed by the energy-momentum conservation equations. In the hadronisation stage, over a small temperature interval, entropy density will decrease very fast. Since total entropy can not decrease, it implies that the fire ball will expand rapidly, while temperature remains approximately constant.

- **Freeze-out:** Hadronic matter will also be in thermal equilibrium. Constituent hadrons will collide to maintain local equilibrium. The system will expand and cool. A stage

will come when inelastic collisions, in which hadron changes identity, become too small to keep up with expansion. This stage is called **chemical freeze-out**. Hadron abundances will remain fixed after the chemical freeze-out. However, due to elastic collisions, local equilibrium can still be maintained and system will cool and expand with fixed hadron abundances. Eventually a stage will comes when average distance between the constituents will be larger than strong interaction range. Collisions between the constituents will be so infrequent that local thermal equilibrium can not be maintained. The hydrodynamic description will break down. The hadrons decouple or freeze-out. It is called **kinetic freeze-out**. Hadrons from the freeze-out surface will be detected in the detector.

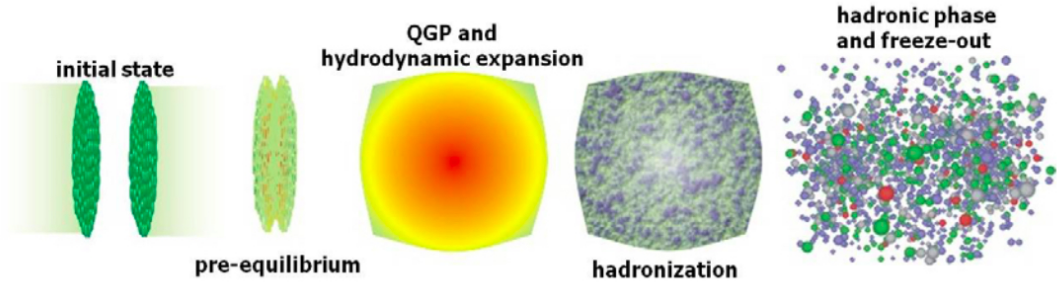

Figure 1.4: Different stages of nuclear collisions. [Luo11]

Note on Hydrodynamics: Hydrodynamics provides a simple, intuitive description of relativistic heavy-ion collisions. Hydrodynamic models requires the assumption of local thermal equilibrium, i.e. at each space time point x of the fluid, a small region can be considered where equilibrium is achieved, a temperature T(x) can be defined. As discussed above, from the equilibrium stage to the kinetic freeze-out, relativistic heavy ion collisions can be modelled by hydrodynamics.

A variety of experimental data from Relativistic Heavy Ion Collider (RHIC) experiments, are successfully explained in ideal hydrodynamical models. Some problems however remain. For example, ideal hydrodynamics description of experimental data becomes poorer as the collisions become more and more peripheral.

1.7 Kinematic Quantities

In dealing with the experimental data on high-energy collisions, one frequently encounters some kinematic variables. These include collision centrality, rapidity and pseudorapidity.

1.7.1 Collision Centrality

The large accelerators like LHC and RHIC collide bunch of particles (nuclei) coming in from opposite directions. When one such particle from one beam scatters off of another particle in the other beam, this is what we define as one event. One very important quantity characterizing any type of collision is the impact parameter b. Small b collisions are called central whereas large impact parameter collisions are called peripheral. The impact parameter of each event varies during the collision. The collection of all possible impact parameters is called a **minimum bias sample**. This variation of impact parameter is called centrality. For example, 0-5$\%$ centrality covers the impact parameter range from 0 to 3.50 fm (for Pb-Pb collisions at $\sqrt{s_{NN}}$ = 2.76 TeV). However, impact parameter is not the only way of characterizing the collision centrality. Centrality can also be defined in terms of the number of participating nucleons (N_{part}), the nucleons that has undergone at least one inelastic collision or in terms of the binary nucleon collision number. The other two parameters have one to one correspondence with the impact parameter which can be calculated in a Glauber Model [MRSS07]. More on this covered in the next chapter.

1.7.2 Rapidity

The rapidity of a particle is defined as

$$y = \frac{1}{2} ln(\frac{E + p_z c}{E - p_z c}) \tag{1.5}$$

where E is the total energy of the particle and p_z is it's longitudinal momentum. Conventionally the z-direction is taken as the beam axis.

Why rapidity is used?

Suppose a particle, in a collision, is predominantly produced along the beam direction say the +z direction. In that case E $\approx p_z c$, so that y $\rightarrow \infty$. If the particle moved along the -z direction, then y $\rightarrow -\infty$. Consider now the particle being produced in a direction perpendicular to the beam axis, so that p_z = 0 and y $\rightarrow$ 0. Thus we see that the rapidity of a particle

is related to the angle at which the particle is produced with respect to the beam direction.

Some calculations on rapidity

$$y = \frac{1}{2} ln(\frac{E + p_z c}{E - p_z c}) = ln(\sqrt{\frac{E + p_z c}{E - p_z c}}) \tag{1.6}$$

$$y = ln(\sqrt{\frac{E + p_z c}{E - p_z c}}) = ln(\frac{E + p_z c}{\sqrt{E - p_z c}\sqrt{E + p_z c}}) = ln(\frac{E + p_z c}{\sqrt{E^2 - p_z c^2}}) \tag{1.7}$$

Using the definition of transverse mass, $M_T^2 c^4 = p_x^2 c^2 + p_y^2 c^2 + M^2 c^4$, where M is the rest mass, we get

$$y = ln(\frac{E + p_z c}{M_T c^2}) \tag{1.8}$$

Now, using the identity

$$tanh\theta = \frac{e^\theta - e^{-\theta}}{e^\theta + e^{-\theta}} \tag{1.9}$$

$$y = tanh^{-1}(tanh(ln(\frac{E + p_z c}{M_T c^2})) \tag{1.10}$$

$$y = tanh^{-1}\Big(\frac{exp(ln(\frac{E+p_z c}{M_T c^2})) - exp(-ln(\frac{E+p_z c}{M_T c^2}))}{exp(ln(\frac{E+p_z c}{M_T c^2})) + exp(-ln(\frac{E+p_z c}{M_T c^2}))}\Big) \tag{1.11}$$

$$y = tanh^{-1}\Big(\frac{\frac{E+p_z c}{M_T c^2} - \frac{M_T c^2}{E+p_z c}}{\frac{E+p_z c}{M_T c^2} + \frac{M_T c^2}{E+p_z c}}\Big) \tag{1.12}$$

Using simple algebra we finally get

$$y = tanh^{-1}\Big(\frac{p_z c(E + p_z c)}{E(E + p_z c)}\Big) \tag{1.13}$$

$$y = tanh^{-1}\Big(\frac{p_z c}{E}\Big) \tag{1.14}$$

Rapidity transformation under Lorentz Boosts parallel to the beam direction: For this we first need to see how the components of 4-momentum transforms with respect to boosts along the z direction:

$$E^{'}/c = \gamma(E/c - \beta p_z) \tag{1.15}$$

$$p_x^{'} = p_x \tag{1.16}$$

$$p_y^{'} = p_y \tag{1.17}$$

$$p_z^{'} = \gamma(p_z - \beta E/c) \tag{1.18}$$

Substituting this into the equation above

$$y^{'} = \frac{1}{2} ln\Big(\frac{\gamma E/c - \beta\gamma p_z + \gamma p_z - \beta\gamma E/c}{\gamma E/c - \beta\gamma p_z - \gamma p_z + \beta\gamma E/c}\Big) \tag{1.19}$$

$$y^{'} = \frac{1}{2} ln\Big(\frac{(E/c + p_z)(\gamma(1-\beta))}{(E/c + p_z)(\gamma(1+\beta))}\Big) \tag{1.20}$$

$$y^{'} = \frac{1}{2} ln(\frac{E + p_z c}{E - p_z c}) + ln(\sqrt{\frac{1-\beta}{1+\beta}}) \tag{1.21}$$

$$y^{'} = y + ln(\sqrt{\frac{1-\beta}{1+\beta}}) \tag{1.22}$$

This expression can further be simplified

$$ln(\sqrt{\frac{1-\beta}{1+\beta}}) = tanh^{-1}(tanh(ln(\sqrt{\frac{1-\beta}{1+\beta}}))) \tag{1.23}$$

$$= tanh^{-1}\Big(\sqrt{\frac{\frac{1-\beta}{1+\beta} - \frac{1-\beta}{1+\beta}}{\frac{1-\beta}{1+\beta} + \frac{1-\beta}{1+\beta}}}\Big) \tag{1.24}$$

$$= tanh^{-1}\beta \tag{1.25}$$

Thus we finally get from above equations

$$y^{'} = y - tanh^{-1}\beta \tag{1.26}$$

Suppose there are two particles flying out of the collision region with rapidities y_1 and y_2 as measured by some observer. Now let some other observer measure the same rapidities from a different frame of reference and get $y_1^{'}$ and $y_2^{'}$.

$$y_1^{'} - y_2^{'} = y_1 - tanh^{-1}\beta - y_2 + tanh^{-1}\beta = y_1 - y_2 \tag{1.27}$$

Thus the difference between the rapidities of two particles is invariant with respect to boosts along the beam direction. This is why rapidity is so important in accelerator physics.

1.7.3 Pseudo-rapidity

For outgoing particles with very high p_z values, it can be very difficult to measure the p_z value precisely because the beam pipe can be in the way of measuring it and hence the rapidity can be hard to measure for such particles. However we can define a quantity that is almost the same thing as rapidity but can be determined much easily than rapidity for highly energetic particles. The quantity is called pseudo-rapidity (η). Starting with the definition of rapidity

$$y = \frac{1}{2} ln(\frac{E + p_z c}{E - p_z c}) \tag{1.28}$$

$$y = \frac{1}{2} ln(\frac{\sqrt{p^2c^2 + m^2c^4} + p_z c}{\sqrt{p^2c^2 + m^2c^4} - p_z c}) \tag{1.29}$$

For a highly relativistic particle pc $<< mc^2$

$$y = \frac{1}{2} ln\Big(\frac{pc(1 + \frac{m^2c^4}{p^2c^2}) + p_z c}{pc(1 + \frac{m^2c^4}{p^2c^2}) - p_z c}\Big) \tag{1.30}$$

$$y \approx \frac{1}{2} ln\Big(\frac{pc + p_z c + \frac{m^2c^4}{2pc} + ...}{pc + p_z c + \frac{m^2c^4}{2pc} + ...}\Big) \tag{1.31}$$

$$y \approx \frac{1}{2} ln\Big(\frac{1 + \frac{p_z}{p} + \frac{m^2c^4}{2pc} + ...}{1 + \frac{p_z}{p} - \frac{m^2c^4}{2pc} + ...}\Big) \tag{1.32}$$

Now $\frac{p_z}{p} = cos\theta$, where θ is the angle made by the particle trajectory with the beam pipe.

$$1 + \frac{p_z}{p} = 1 + cos\theta = 2cos^2\frac{\theta}{2} \tag{1.33}$$

$$1 - \frac{p_z}{p} = 1 - cos\theta = 2sin^2\frac{\theta}{2} \tag{1.34}$$

Substituting these back into the above equation we get

$$y \approx -ln(tan\frac{\theta}{2}) \tag{1.35}$$

Thus we define pseudo-rapidity as

$$\eta = -ln(tan\frac{\theta}{2}) \tag{1.36}$$

Thus we see that the quantity η is directly related to the angle at which the particle is emitted with respect to the beam direction and hence is much easier to calculate.

Chapter 2

Techniques to probe the QGP

2.1 Signals of Quark-Gluon-Plasma

In the final state of heavy-ion collisions, the detector detects some thousands of particles produced in the collision. The deconfined medium of quarks and gluons exist for only a few microseconds. It is extremely difficult to directly observe QGP in this short lifetime. However, the various particles produced in the collision might prove to be useful as signatures of QGP. There may be no unique signal which will lead to the identification of QGP. The problem is closely related to quark confinement; quarks are unobservable. QGP, even if produced in a collision, is a transient state, it expands, cools, hadronises, cools further till interactions between the hadrons become too weak to continue the evolution. Any information about the QGP phase, if produced in high energy nuclear collisions, has to be obtained from the observed hadrons only. Instead, a number of different signals come out from the medium which may be treated as QGP signatures. Present search for QGP at RHIC/LHC is on the premise that the hadronisation process does not erase the memory and from the observed hadrons, one can comment on the possible existence of QGP. An account of some of these signatures is given below:

2.1.1 J/Ψ suppression

Firstly we define what quarkonia are, they are made up of $c\overline{c}$ and $b\overline{b}$ pairs (c = charm quark, b = bottom quark) that are created in the initial phase of the collision, Color screening in the deconfined phase leads to melting of quarkonia states. The freed c and b quarks are unlikely to recombine to quarkonia states during freeze-out if their concentrations are too

low. Quarkonium mass, radius and formation time can be obtained from the solution of non-relativistic Schrodinger equation and are given in the Figure 2.1.

In 1986, Matsui and Satz suggested that if QGP is formed in nuclear collisions, J/Ψ, the bound state of $c\bar{c}$ will be suppressed, w.r.t. pp collisions. The idea is simple. In presence of QGP, J/Ψ production will be inhibited due to screening of potential. A $c\bar{c}$ pair, which could transform into a J/Ψ, is now unable to do so. Over the years, several groups have measured the J/Ψ, yield in heavy ion collisions. In brief, experimental data do show suppression. However, suppression is observed in pA collisions also, where, one does not expect QGP formation. It is understood that in an inelastic collision with nucleons, J/Ψ's can be dissociated and lead to suppression. Suppression in pA collisions is termed cold nuclear matter (CNM) effect. It is important to disentangle CNM effect from the experimental data to obtain the suppression due to deconfinement.

state	J/ψ	χ_c	ψ'	Υ	χ_b	Υ'	χ_b'	Υ''
mass [GeV]	3.10	3.53	3.68	9.46	9.99	10.02	10.26	10.36
ΔE [GeV]	0.64	0.20	0.05	1.10	0.67	0.54	0.31	0.20
ΔM [GeV]	0.02	-0.03	0.03	0.06	-0.06	-0.06	-0.08	-0.07
r_0 [fm]	0.50	0.72	0.90	0.28	0.44	0.56	0.68	0.78

Figure 2.1: Quarkonium Spectroscopy from Non-Relativistic Potential Theory [Sat06]

2.1.2 Strangeness Enhancement

The ratio of s, u quarks do not show a significant $\sqrt{s}$ dependence in p-p collision. Contrarily, the number of strange particles are enhanced in heavy-ion collision. This is explained by the lower threshold energy of the production of strange particles in deconfined matter compared to hadronic matter, the effective masses of the quarks change from constituent masses in hadronic matter to bare masses in deconfined matter [GO09].

As an example the associated production of strange particles and quarks can be compared, in hadronic matter the lightest strange particle is the kaon, thus the production of a kaon

pair has a threshold energy of about 987 MeV. In the deconfined medium the production of an $s\overline{s}$ pair has a threshold of only about 140 - 260 MeV and the strange quark content is expected to reach equilibrium quickly. However, if strange quarks are produced at a late stage in the expansion of a fluid initially dominated by gluons, the net strangeness will again be greatly reduced on sufficiently small rapidity scale. Consequently, fluctuations in net/total strangeness would be reduced/enhanced [TW02].

2.1.3 Flow

In case of non-zero impact parameter collisions, the overlap region of two nuclei is called reaction or participant zone. The initial reaction zone posses azimuthal anisotropy. Multiple collisions among the constituent particles translate this spatial anisotropy into the momentum anisotropy of the produced particles. This observed momentum anisotropy is known as the collective flow. Mathematically, the observed momentum anisotropy is defined as the fourier expansion of Lorentz invariant differential yield in the angle ϕ given by:

$$E\frac{d^3N}{d^3p} = \frac{1}{2\pi}\frac{dN}{p_T dp_T dy}[1 + \sum_{n=1}^{\infty} 2v_n cosn\phi] \tag{2.1}$$

Where ϕ is the azimuthal angle of the detected particle and v_n are called the flow coefficients. v_1 is called directed flow, v_2 is called elliptic flow, v_3 is called triangular flow and so on. Additionally, elliptic flow occurs in non-central collisions due to the asymmetric, almond shaped, collision region which results in an anisotropic expansion. This effect is self-quenching in the sense that the expansion reduces the anisotropy and thus the elliptic flow. Therefore, the measurement of elliptic flow carries signatures of the earlier collision stages [KH04]. The analysis of transverse momentum spectra at central rapidity with respect to the reaction plane in an event allows elliptic flow occurring in the collision to be analyzed.

2.1.4 Jet Quenching

In heavy-ion collisions at ultra-relativistic energies, the partons involved in the collisions are violently accelerated. Just like accelerated electric charges emit electromagnetic radiation in the form of photons, accelerated color charges emit QCD radiation in the form of gluons. Photons are not electrically charged but gluons are color charged. Hence gluons

can further emit more gluons or a gluon can decay into a quark-antiquark pair, thus leading to parton showers.

Jets are formed when a parton from a nucleus or nucleon scatters off of a parton from another nucleus or nucleon. After the scattering, the partons form parton showers which then hadronizes leading to a collimated spray of hadrons. Now, if a hot and dense QGP medium is produced in AA collision, then a jet created in early collision will propagate through this medium. Due to interaction with the medium, the jet particles will dissipate some energy while propagating through the medium. Usually, in experiments, the transverse momentum distribution of the particles produced in heavy-ion collisions is studied. The energy loss by the jet particles will result in a suppression of the high-pT particles and is commonly known as jet quenching [GP90]. Mathematically, jet quenching is measured through a quantity defined as Nuclear Modification Factor (R_{AA}). It is defined as:

$$R_{AA} = \frac{\frac{dN_{AA}}{d^2p_T dy}}{T_{AA}\frac{d\sigma_{AA}}{d^2p_T dy}} \tag{2.2}$$

The numerator is the single particle transverse momentum distribution of a jet parton produced in AA collision and travelling through the hot and dense QGP medium. The denominator shows single particle distribution of same species of jet parton produced in p-p collision multiplied by nuclear thickness function T_{AA} which is a proton to nucleus scaling factor (if AA collision is an incoherent superposition of p-p collision) and is a function of impact parameter b. A value of R_{AA} equals to 1 indicates that no jet quenching has taken place. However if the ratio tends to be less than unity, it serves as a definite measure for jet suppression in the medium and thus serves as a signature for QGP.

The back-to-back correlation that can be usually observed in two-jet events due to momentum conservation in the hard parton-parton interaction is strongly influenced by the medium. This correlation is broadened; one jet may even be completely absorbed. Jet production rates measured in p-p collisions, again, provide an essential reference here.

2.1.5 Identical Particle Interferometry

Two (or more) particle momentum correlations reveal information about the space-time dynamics of the collision. This procedure is analogous to Hanbury-Brown and Twiss (HBT) interferometry that has been successfully used in astrophysics to determine the angular diameter of stars. In high-energy physics these correlations allow the size, lifetime, and

flow patterns of the fireball at the moment when the hadronization occurs to be measured. The three-particle interferometer is another viable candidate for revealing such information on space-time dynamics.

2.1.6 Dilepton and Photon Spectra

Leptons and photons are produced throughout the entire evolution of the collision. However, leptons and photons produced in the earliest and hottest phase of the collision do not interact strongly with the fireball. Therefore, they are a probe of the phase at its highest temperature. In the measurement, both of them are dominated by large backgrounds from hadronic processes, for example from pions, kaons, ρ and π^0 . The yields of dileptons and photons are compared between heavy-ion and p+p collisions to extract signals from the early collision phase.

Dileptons are a signal of medium modifications of hadronic matter, e.g. of the mass of the ρ-meson. Furthermore, dileptons from charm decay allow the total charm yield to be accessed, which is important for the measurement of the total production cross-section of the J/Ψ.

2.1.7 Chiral-Symmetry Restoration

The Lagrangian of QCD implies approximate chiral symmetry. As a consequence the baryon number should be conserved for right- handed and left-handed quarks separately. In nature only the total baryon number is conserved thus chiral symmetry is broken. The symmetry breaking is twofold: to start with the symmetry is only approximate due to the finite, however small, bare quark masses that cause a so-called explicit symmetry breaking. Furthermore, the quarks acquire their constituent masses in the interaction with the QCD vacuum at low T which is a spontaneous breaking of the symmetry [PP00]. It is predicted that the spontaneous breaking of chiral-symmetry is restored at temperatures prevailing in the QGP phase. As a consequence the position and width of the masses of the light vector mesons (ρ, ω, and ϕ) may change (see e.g. [Pis82]). Indications have been seen at the SPS [AAA$^+$03] [DC$^+$07].

A central aspect of the ALICE research program is to analyze heavy-ion collisions to strengthen the evidence for the existence of the QGP, to study its properties as well as

the phase transition between hadronic matter and the plasma. As outlined above many of the signatures require a solid p+p reference. Therefore, the measurement of p+p collisions is crucial for the study of the QGP and the phase transition. It should be pointed out that the measurements of p+p collisions at $\sqrt{s}$ = 10 TeV or $\sqrt{s}$= 14 TeV cannot be directly used as reference for Pb+Pb collisions that will be performed at $\sqrt{s}_{NN}$ of 5.5TeV. Instead the measurements at high energies are used to interpolate to the energy in heavy-ion collisions.Ultimately, the measurement of p+p collisions at $\sqrt{s}$ = 5.5 TeV is the preferred reference.

One of the spectacular predictions of quantum chromodynamics (QCD) is that at extremely high density and/or temperature the hadronic matter undergoes a phase transition to QGP. Heavy-ion collisions at relativistic energies offer a unique environment for the creation and study of the QGP phase in the laboratory. A characteristic feature of this process is that the system experiences large event by event fluctuations in thermodynamic quantities such as temperature and entropy. These can be studied by the experimentally observed quantities such as fluctuations of mean transverse momentum and multiplicity.

2.2 Event by Event Fluctuations

The importance of Event by Event fluctuations can be emphasized using this example, if we keep a sheet of paper in rain and let it get wet for some time(corresponding to averaging) the paper would get wet uniformly and we can conclude that the rain was of uniform type. Although if we kept multiple sheets of paper at intervals of few seconds then we could see different splatter patterns of rain and also whether it hailed or snowed in between the rain. So analyzing many events not only gives us better statistics but also may reveal rare events like even a phase transition. This is why Event by Event fluctuations matter.

2.2.1 Net Charge Fluctuations:

In the formalism of grand canonical ensemble, for a system of classical ideal gas, net charge fluctuations are proportional to the square of electric charge which takes up distinct values for the QGP and hadronic phases. While the unit of charge in the hadronic phase is 1, in the QGP phase it is 1/3. However, the fluctuation in the net charge depends on the squares of the charges and hence strongly depends on which phase it originates from though the net

charge doesn't depend on such subtleties [C$^+$12]. Measuring the charge fluctuation itself, however, is plagued by systematic uncertainties such as volume fluctuations due to the impact parameter variation. The task for us is then to find a suitable ratio whose fluctuation is easy to measure and simply related to the net charge fluctuation.
We can write the fluctuations of net charge as:

$$\langle \delta Q^2 \rangle = q^2 \langle (\delta p - \delta n)^2 \rangle \tag{2.3}$$

where q is the charge of the particles in the system, p is the number of positively charged particles and n is the number of negatively charged particles in the system.
Using thermal distributions and disregarding correlations, we get:

$$\langle \delta Q^2 \rangle = q^2 (\langle \delta n^2 \rangle + \langle \delta p^2 \rangle) \tag{2.4}$$

In limit of very high temperature, both Bose-Einstein and Fermi-Dirac statistics reduces to the classical Maxwell-Boltzmann statistics. Moreover, at extremely high temperatures or energy densities, due to asymptotic freedom, quark interactions are very weak and we can approximate the hot and dense medium formed in heavy-ion collisions as a classical ideal gas.
For the case of a classical ideal gas in grand canonical ensemble, we have fluctuation in a quantitiy N as [Appendix A]:

$$\langle N^2 \rangle - \langle N \rangle^2 = \langle N \rangle \tag{2.5}$$

Using this result and equation above:

$$\langle \delta Q^2 \rangle = q^2 (\langle n \rangle + \langle p \rangle) \tag{2.6}$$

$$\langle \delta Q^2 \rangle = q^2 \langle N \rangle \tag{2.7}$$

where N = n+p is the total number of charged particles. Using this relation and the principle outlined above, the measurement of net charge fluctuations can serve as a definite measure for the formation of QGP in heavy-ion collisions.

The numbers of particles produced in relativistic nuclear collisions differ dramatically from collision to collision due to the variation of impact parameter, energy deposition, baryon stopping and other dynamical effects. Such fluctuations can also be influenced

by novel phenomena such as disoriented chiral condensate or the appearance of multiple event classes. Even globally conserved quantities such as net charge, baryon number and strangeness can fluctuate when measured, e.g., in a limited rapidity interval. The rapid hadronization of a quark-gluon plasma (QGP) can reduce net charge fluctuations compared to hadronic expectations, while phase separation can increase net-baryon fluctuations. Fluctuations of conserved quantities are possibly the best probes of such novel dynamics, because conservation laws limit the degree to which final-state scattering can dissipate them [PGV02].

2.2.2 Transverse Momentum Fluctuations

Fluctuations in average transverse momentum were among the first event-by- event analyses studied. In a series of papers Mrowczynski et al have tried to the degree of thermalization by studying transverse momentum fluctuations.Experimental analyses by NA49 [Tra00] reveal that a careful evaluation of systematic effects are required before substantial equilibration can be claimed in central heavy-ion collisions from transverse momentum fluctuations. They also have found strong correlations between multiplicity and transverse momentum.
There are numerous observables that can be used to measure p_T fluctuations, the most obvious one being is the distribution of average transverse momentum:

$$M(p_T) = \frac{1}{N}\sum_{i=1}^{N} p_{T_i} \tag{2.8}$$

where N is the multiplicity of accepted particles in a given event and p_{T_i} is the transverse momentum of the i^{th} particle.
The distribution of $M(??p_T)??$ is usually compared to its corresponding distribution obtained for mixed events in which the particles are independent from each other and follow the experimental inclusive spectra (the multiplicity distribution for mixed events is the same as for the data). A difference between the two distributions signals the presence of dynamical fluctuations[ABB$^+$04].
Another quantity used to measure transverse momentum fluctuations is Φ_{p_T}, following the authors of [GM92] one defines the single particle variable $z_{p_T} = p_T - \overline{p_T}$ with the bar denoting averaging over the single particle inclusive distribution. Then Z_{p_T} is defined which

the multiparticle analog of z_{p_T} defined as:

$$Z_{p_T} = \sum_{i=1}^{N} (p_T - \overline{p_T}) \tag{2.9}$$

Note that $< Z_{p_T} >$ = 0. Finally the Φ_{p_T} quantity is defined as:

$$\Phi_{p_T} = \sqrt{\frac{< Z_{p_T}^2 >}{< N >}} - \sqrt{\overline{z_{p_T}^2}} \tag{2.10}$$

Φ by its construction, is insensitive to the system size and is insensitive to centrality.

Chapter 3

Higher Moments and ν dynamics

In this section we discuss about the probes used for quantifying the fluctuations in the system, ν Dynamics is used for finding if there are any dynamical fluctuations that can be accounted for new physics taking place. The Higher Order moments are for quantifying this new fluctuations by comparing with Statistical systems which we already know about.

3.1 Moments Methodology in Heavy Ion Collision

In this work we are focusing on, how to deal with the charged multiplicity distribution of heavy ion collisions. From section 2.1, one can get the idea about, how the out coming particles are important in the study of heavy ion physics. Since we do not have the information about the system formed during the collision, these multiplicity tracks are the pathway which carries the information about the system which we are interested in.

In statistics, moments are used to characterize the shape of a probability distribution. For example, the second central moment (moment about the mean), variance (σ^2) is widely applied to describe the width of a probability distribution. The skewness (S) and kurtosis (κ) are used to describe how the distributions skewed and peaked from its mean value, respectively. Another alternative method to the moments of a distribution are the so called cumulants. The cumulants determine the moments in the sense that any two probability distributions whose cumulants are identical will have identical moments as well, and similarly the moments determine the cumulants. In heavy ion collision, the higher moments of distributions of conserved quantities, such as net-baryon, net-charge and net-strangeness, are predicted to be sensitive to the correlation length and to be connected to the thermody-

namic susceptibilities computed in Lattice QCD [GG11] and in the Hadron Resonance Gas (HRG) [KR11] model.

3.2 Cumulants and Moments

3.2.1 Definition

In probability theory and statistics, the cumulants of a probability density distribution can be defined by using the cumulant-generating function [Hal00]. The cumulant-generating function of the random variable X is defined as:

$$G(t) = log[E(e^{tX})] \tag{3.1}$$

where the E is the expectation operator and some times denoted by angle brackets $\langle\,\rangle$, E(e^{tX}) = $\langle e^{tX} \rangle$ = $\int_{-\infty}^{+\infty} e^{tX} f(X) dX$, for a real-valued continuous probability density function f(x). Generally, the nth order cumulants C_n can be extracted from the cumulant-generating function via differentiation (at zero) of G(t).

$$C_n = G^n(0) = \frac{\partial^n G(t)}{\partial t^n}|_{t=0} \tag{3.2}$$

Cumulants of a distribution are closely related to the moments of the distribution and the moment-generating function for moments about zero can be written as:

$$g(t) = E(e^{tX}) = 1 + \sum_{n=1}^{\infty} \langle X^n \rangle \frac{t^n}{n!} \tag{3.3}$$

Consequently the n^{th} order moments about zero $\mu_n = \langle X^n \rangle$ can be obtained by:

$$\mu_n = \langle X^n \rangle = g^n(0) = \frac{\partial^n g(t)}{\partial t^n}|_{t=0} \tag{3.4}$$

Thus, the cumulant-generating function can be expressed in term of the moments about zero as:

$$G(t) = log[g(t)] = -\sum_{n=1}^{\infty} \frac{1}{n}(1 - g(t))^n = \sum_{n=1}^{\infty} \frac{1}{n}(-\sum_{m=1}^{\infty} \mu_m \frac{t^m}{m!})^n \tag{3.5}$$

$$= \mu_1 \times t + (\mu_2 - \mu 1^2) \times \frac{t^2}{2!} + (\mu_3 - 3\mu_2\mu_1 + 2\mu_1^3) \times \frac{t^3}{3!} + ... \tag{3.6}$$

Finally, we obtain the connections between the cumulants, moments about zero $\mu_n$and central moments (moments about mean) $\mu_n^{'} = \langle (X - \langle X \rangle)^n \rangle = \langle (\delta X)^n \rangle$:

$$C_1 = \mu_1 = \langle X \rangle \tag{3.7}$$

$$C_2 = \mu_2 - \mu 1^2 = \langle (X - \langle X \rangle)^2 \rangle \tag{3.8}$$

$$C_3 = \mu_3 - 3\mu_2\mu_1 + 2\mu_1^3 = \langle (X - \langle X \rangle)^3 \rangle \tag{3.9}$$

$$C_4 = \mu_4 - 4\mu_3\mu_1 - 3\mu 2^2 + 12\mu_2\mu_1^2 - 6\mu_1^4 \tag{3.10}$$

$$= \langle (X - \langle X \rangle)^4 \rangle - 3 \times (\langle (X - \langle X \rangle)^2 \rangle)^2 \tag{3.11}$$

.

.

.

$$C_n = \mu_n - \sum_{m=1}^{n-1} \binom{n-1}{m-1} C_m \mu_{n-m} \tag{3.12}$$

$$= \mu_n^{'} - \sum_{m=1,(n-m,n\geq 2)}^{n-1} \binom{n-1}{m-1} C_m \mu_{n-m}^{'} \tag{3.13}$$

Usually, the central moments are more useful than the moments about zero to describe the shape of the distributions. The second central moment (variance (σ^2)) is used to describe the width of a distributions. The normalized third central moment and forth central moment so called skewness (S) and kurtosis (κ), are used to describe the asymmetry and how peaked the distributions are, respectively. They are defined as:

$$\sigma^2 = \langle (X - \langle X \rangle)^2 \rangle = C_2 \tag{3.14}$$

$$S = \frac{\langle (X - \langle X \rangle)^3 \rangle}{\sigma^3} = \frac{C_3}{(C_2)^{3/2}} \tag{3.15}$$

$$\kappa = \frac{\langle (X - \langle X \rangle)^4 \rangle}{\sigma^4} - 3 = \frac{C_4}{(C_2)^2} \tag{3.16}$$

Fig. 3.1 gives a visual example for determining which of the two kinds of skewness a distribution has. The distribution shown in the left panel, which gives negative skewness, is said to be left-skewed. It has a longer left tail and the center of the distribution is concentrated on the right of the distribution. The distribution in the right panel of Fig. 3.1 shows you a distribution with positive skewness, which is said to be right-skewed. It has a longer right tail and the center of the distribution is concentrated on the left of the distribution. A zero value indicates that the values are relatively evenly distributed on both sides of the mean, typically but not necessarily implying a symmetric distribution.

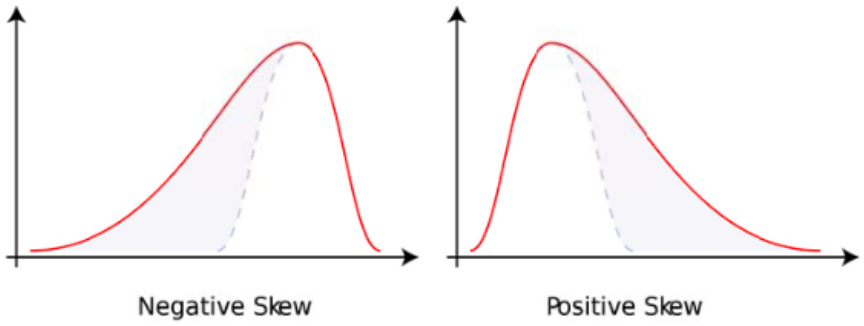

Figure 3.1: Visual example of distribution with negative skewness (left panel) and positive skewness (right panel).

It is found that the distributions with a sharp peak have a larger kurtosis value than those distributions with broad tails. A high kurtosis distribution has a sharper peak and longer, fatter tails, while a low kurtosis distribution has a more rounded peak and shorter thinner tails. The kurtosis must be at least -2, which can be realised by the Bernoulli distribution with p = 1/2. There is no upper limit to the kurtosis and it may be infinite. For normal distributions, both, the skewness and the kurtosis are equal to zero. Thus, they are ideal probes of the non-gaussian fluctuations.

3.2.2 Applications in Heavy Ion Collision

Experimentally, we measure particle multiplicities event-by-event wise. In the following, we use N to represent the particle number in one event. The average value over the whole event ensemble is denoted by $\langle N \rangle$, where the single angle brackets are used to indicate ensemble average of an event-by-event distributions.
The deviation of N from its mean value is defined by:

$$\delta N = N - \langle N \rangle \tag{3.17}$$

Then, we can define the various order cumulants of event-by-event distributions of a variable N.

$$C_1 = \langle N \rangle \tag{3.18}$$

$$C_2 = \langle (\delta N)^2 \rangle \tag{3.19}$$

$$C_3 = \langle (\delta N)^3 \rangle \tag{3.20}$$

$$C_4 = \langle(\delta N)^4\rangle - 3\langle(\delta N)^2\rangle^2 \tag{3.21}$$

Once we have the definition of cumulants, various moments can be denoted as:

$$M = C_1 \tag{3.22}$$

$$\sigma^2 = C_2 \tag{3.23}$$

$$S = \frac{C_3}{(C_2)^{3/2}} \tag{3.24}$$

$$\kappa = \frac{C_4}{(C_2)^2} \tag{3.25}$$

And also, the moments product $\kappa\sigma^2$ and $S\sigma$ can be expressed in terms of cumulant ratios.

$$\kappa\sigma^2 = \frac{C_4}{C_2}; S\sigma = \frac{C_3}{C_2} \tag{3.26}$$

With above definition of various moments, we can calculate various moments and moment products with the measured event-by-event particle number fluctuations in a certain p_T and rapidity range for each centrality. Higher moments of conserved quantities, such as net-baryon, net-charge and net-strangeness number are predicted to be sensitive to the correlation length developed in heavy ion collisions and are directly linked to the thermodynamic susceptibilities computed in Lattice QCD and in the Hadron Resonance Gas (HRG) model.

The window in rapidity should be at least about one unit wide, in order for the results to apply without significant acceptance corrections. Furthermore, the longitudinal expansion of the matter produced in the collision reduces correlations among particles separated by much more than one unit in rapidity, making larger windows unnecessary.

In statistics, skewness and kurtosis are widely used to characterize the properties of probability distributions. Skewness is used to describe the asymmetry property of distributions, while kurtosis describes how peaked they are. Sign changing of skewness as a function of colliding energy may indicate a crossing of phase boundary. In addition, for normal distributions, both of the skewness and kurtosis are equal to zero, thus they are ideal probe of non-Gaussian fluctuations.

3.2.3 Expectations from Poisson Statistics

Many background effects result in statistical fluctuations, which obey the Poisson statistics. If we assume our true signals are not correlated with those statistical backgrounds, then

the Poisson value of our observables can serve as a baseline. In statistics, the probability distribution of Poisson can be expressed as:

$$P(X = k) = \frac{e^{-\lambda}\lambda^k}{k!} \tag{3.27}$$

where k is the random variable and λ is the parameter of the Poisson distribution. The various moments (M, σ, S, κ) as well as moment products $(\kappa\sigma^2, S\sigma)$ of single Poisson distribution are simple :

$$M = \lambda \tag{3.28}$$

$$\sigma = \sqrt{\lambda} \tag{3.29}$$

$$S = \frac{1}{\sqrt{\lambda}} \tag{3.30}$$

$$\kappa = \frac{1}{\lambda} \tag{3.31}$$

$$\kappa\sigma^2 = S\sigma = 1 \tag{3.32}$$

Hence, for particle multiplicities, its Poisson value of its various moments are simple. In our case, we are dealing with the difference of two independent Poisson distributions, such as net-proton, net-charge. The difference of two independent Poisson distributions distributed as the so called Skellam distributions. Its probability density formula is :

$$f(k : \mu_1, \mu_2) = e^{-\mu_1+\mu_2}(\frac{\mu_1}{\mu_2})^{k/2} I_{|k|}(2\sqrt{(}\mu_1\mu_2) \tag{3.33}$$

where μ_1 and μ_2 are the mean value of two Poisson distributions, respectively, the $I_k(z)$ is the modified Bessel function of the first kind. Then, we can calculate various moments (M, σ, S, κ) and moment products $(\kappa\sigma^2, S\sigma)$ products of the Skellam distribution. The results are shown below:

$$M = \mu_1 - \mu_2 \tag{3.34}$$

$$\sigma = \sqrt{(}\mu_1 + \mu_2) \tag{3.35}$$

$$S = \frac{\mu_1 - \mu_2}{(\mu_1 + \mu_2)^{3/2}} \tag{3.36}$$

$$\kappa = \frac{1}{\mu_1 + \mu_2} \tag{3.37}$$

$$S\sigma = \frac{\mu_1 - \mu_2}{(\mu_1 + \mu_2)} \tag{3.38}$$

$$\kappa\sigma^2 = 1 \tag{3.39}$$

We may find that the $\kappa\sigma^2$ are always unity for both Poisson and Skellam distributions while the $S\sigma$ is changed from unity in Poisson to the above mentioned quantity to describe the asymmetry between μ_1 and μ_2 in Skellam distribution. In our case, if we say the net-charge multiplicity obeys the Poisson statistics, then the positive particles and negative particles should be distributed as independent Poisson distributions and the net-charge multiplicity obeys the Skellam distribution.

3.3 Centrality Determination

The centrality of nucleus-nucleus collisions is an important parameter in heavy ion collision physics. It can be defined by several different parameters. The most common one is the so called impact parameter b, defined as the distance between the geometrical centers of the colliding nuclei in the plane transverse to their direction. Other geometry variables include the number of nucleons that participate, N_{part} and the number of binary collisions, N_{coll}. The number of participants is defined as the number of nucleons, which undergo at least one inelastic nucleon-nucleon collision and the number of binary collisions is defined as number of inelastic nucleon-nucleon collisions. With the above geometric information, we can compare centrality dependence (N_{part}, N_{coll}) of observables between different experiments. Unfortunately, those geometry observables can?t be directly measured and must be deduced from a combination of experimentally measured quantities and Monte-Carlo simulations. This usually is done by a purely geometric model, the so called Glauber model [MRSS07].

In the Glauber model, a nucleus-nucleus collision is treated as a sequences of independent binary nucleon-nucleon collisions. Experimental observables, such as particle multiplicity, not only reflect the geometry of the collision, but also depend on physical processes. This indicates that relation between measured observables and impact parameter does not have a one-to-one correspondence. There are fluctuations for the observable even with a fixed impact parameter. One value of observable may correspond to many possible impact parameters. Experimentally, the centrality is usually expressed as a percentage of the total cross-section, such as 0-5$\%$ (most central), 30-50$\%$ (semi-peripheral), which indicates the fraction of a data sample (corrected for inefficiency) relative to all possible collision geometries (impact parameters).

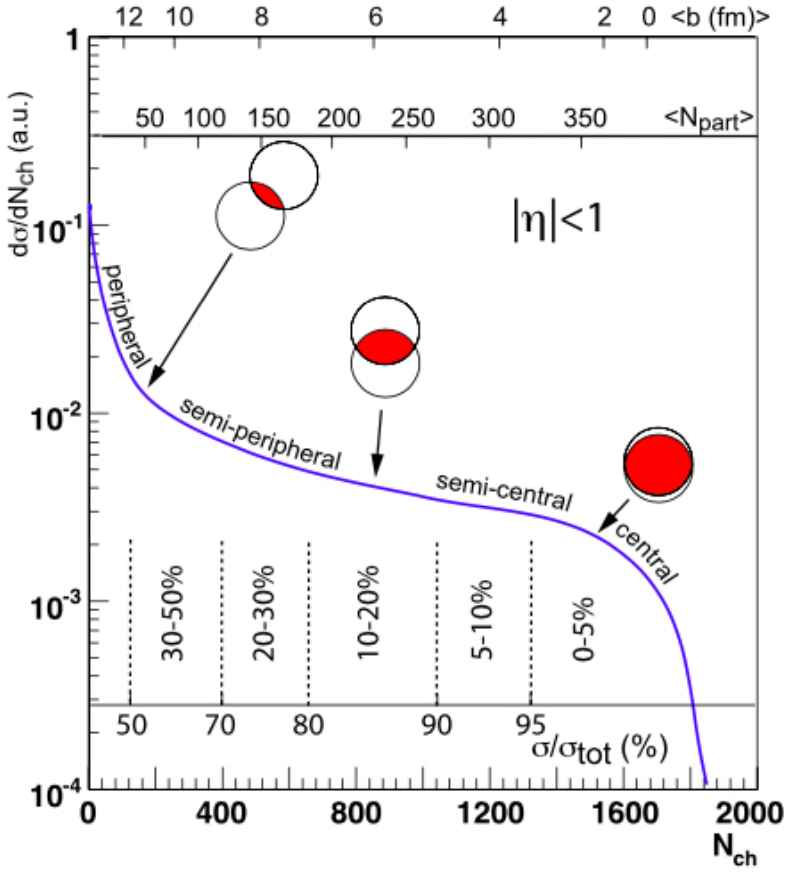

Figure 3.2: A cartoon example of the correlation of the final state observable N_{ch} with Glauber calculated quantities (b, N_{part}). The plotted distribution and various values are illustrative and not actual measurements [MRSS07].

For illustrative purposes, Fig. 3.2 shows a typical centrality determination plot with charged particle multiplicity. Once the total integral of the distribution is known, centrality classes are defined by binning the distribution on the basis of the fraction of the total integral, which is represented by the dashed lines shown in Fig. 3.2. In an analogous way, we can calculate the charged particle multiplicity and determine the centrality classes with Glauber model simulations, in which the average geometrical parameters (N_{part} and N_{coll}) for each centrality bin can be also calculated.

The basic assumption underlying centrality classes is that the impact parameter b is monotonically related to particle multiplicity, both at mid and forward rapidity. For large b events (peripheral) we expect low multiplicity at mid-rapidity, and a large number of spectator nucleons at beam rapidity, whereas for small b events (central) we expect large multiplicity at

mid-rapidity and a small number of spectator nucleons at beam rapidity.

3.4 The quantity ν Dynamics in Heavy Ion Collisions

Multiplicity Fluctuations are driven by intrinsic 2-particle correlations and such a 2-particle co-relator is the quantity called ν dynamics. It was developed to isolate the potentially interesting net-charge fluctuations from factors that cause the numbers of positive and negative hadrons to fluctuate together, such as variations in energy deposition or collision volume. ν Dynamics is both robust and straight forwardly related to the microscopic co-relators it is what gives an estimate about the fluctuations in the system which have a dynamical source because the statistical error was subtracted before hand to get ν Dynamics. ν stat is the error owed to statistical fluctuations its the error in the Poissonian limit which is associated with independent particle production[PGV02].
The quantities are defined as:

$$\nu_{a,b,Dynamic} = \frac{< N_a(N_a-1) >}{< N_a >^2} + \frac{< N_b(N_b-1) >}{< N_b >^2} - 2\frac{< N_a N_b >}{< N_a >< N_b >} \tag{3.40}$$

$$\nu_{a,b,stat} = \frac{1}{< N_a >} + \frac{1}{< N_b >} \tag{3.41}$$

Another form in which ν dynamics is written is as:

$$\nu_{n,p,Dynamic} = R_{pp} + R_{nn} - 2R_{np} \tag{3.42}$$

$$R_{pp} = \frac{< p(p-1) >}{< p >^2} \tag{3.43}$$

$$R_{nn} = \frac{< n(n-1) >}{< n >^2} \tag{3.44}$$

$$R_{np} = \frac{< np >}{< n >< p >} \tag{3.45}$$

R_{pp}, R_{nn}, R_{np} are the particles co-relators the positive - positive particle co-relator the negative - negative particle co-relator and the negative - positive particle co-relator respectively.

3.5 Statistical Fluctuations

As discussed earlier the aim is to find out the fluctuations in the system to understand whether the formation of QGP is taking place or not. To probe these fluctuations Higher

Order Moments and ν Dynamics have been calculated which will be discussed in the next chapters. Firstly to have a comparison and set the baseline Random fluctuations were generated.
For calculating these Random fluctuations the average positive and negative particle multiplicities were calculated by integrating the p_t curve data from experimental data at $\sqrt{s_{NN}}$ = 2.76 TeV. Since this data is available particle species wise an assumption was made that all the charge in the system is accounted by Pions, Kaons and protons.

So independently they were integrated for and Π^+, K^+ and p would be the total positive charge and Π^-, K^- and $\overline{p}$ would be the total negative charge of the system.
For making it random Gaussian and Poisson Fluctuation were generated with mean as the integrated values, 10 million events were generated and the Higher Order Moments have been calculated and plotted along with ν Dynamics, ν stat and particle co-relators.
These Random Fluctuations will be compared with the UrQMD model generated (MC technique) data's Higher Order Moments and ν Dynamics.

The reason for choosing Gaussian and Poisson distributions as sources of Random Fluctuations are because Poisson distribution can be obtained as the limit of the Negative Binomial Distribution which is obtained as the best fit for multiplicities when we fit the Tsallis Distribution to the p_T graphs. Also the NBD fit doesn't give a proper fit for high multiplicities and since high energies values are usually associated high multiplicities. Hence we follow a Poisson distribution for these high multiplicities. So plotting these graphs would give us an idea how the correlated data has the non-Poissonian fluctuations.
The Gaussian distributions are chosen primarily because any random fluctuation can be modelled by white noise and any statistical fluctuation is of the form of Gaussian.

3.6 UrQMD the Event Generator

The UrQMD(Ultra Relativistic Quantum Molecular Dynamics Model) Event generator is the generator that was used for generating the data that has been worked on in this thesis. The package was installed on the cluster at our lab and events were generated simultaneously for different centrality bins, 2500 event per centrality bin.

As expected the model does not fully accommodate all the physics that is undergone during a collision because there are many new underlying physics yet to be discovered. So then how does it work?

This particular model uses a microscopic transport theory which is formulated from covariant propagation of all types of hadrons on classical trajectories and for randomness there is the stochastic binary scatterings it also uses color string formation and resonance decay. It like other generators is a Monte Carlo simulation which has been modelled from the actual experimental data and here it solves a large set of partial differential equations for trajectories and decays.

Chapter 4

ν Dynamics Analysis

As discussed before ν Dynamics is a robust quantity that gives us very valuable information regarding the dynamical fluctuations of the system.
Here once again the plots of random fluctuations are shown to give us an idea to compare with dynamical fluctuations expected from the generated data.For Poissonian fluctuations each of these terms individually becomes unity. So ν Dynamics would become zero for purely statistical (Poisson) fluctuation and non-zero only in the presence of dynamical fluctuation of any form of origin [and08]. The advantage of this variable is that it is robust against detector efficiency and involves only lowest orders of factorial moments which reduces statistical uncertainties.

4.0.1 Gaussian

Gaussian Fluctuation is calculated for accounting for the fluctuations that would come from the statistical fluctuations.
For a variable which has a gaussian distribution its generated by the formula:

$$P(x;\mu;\sigma) = \frac{1}{\sqrt{2\pi}\sigma} e^{\frac{(x-\mu)^2}{2\sigma^2}} \tag{4.1}$$

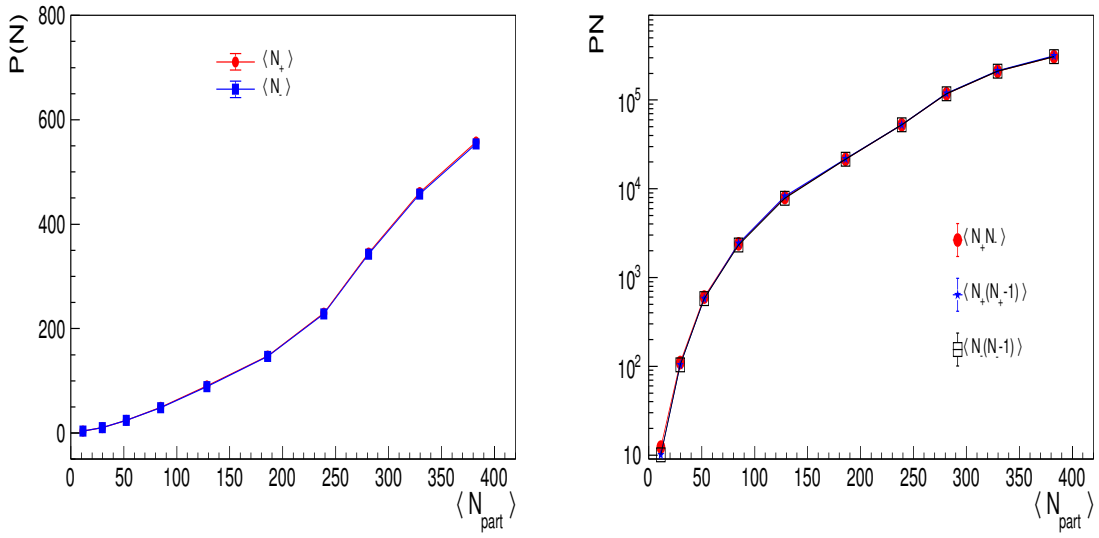

Figure 4.1: On the left we have average values of p and n and on the right we have the factors for choosing two particles if they are same or different.

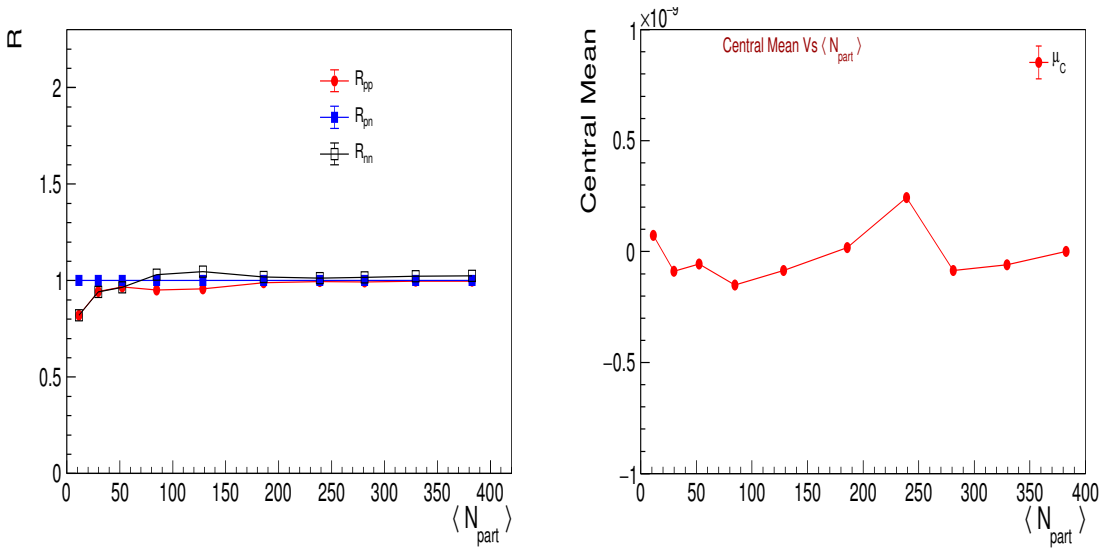

Figure 4.2: On the left we have particle correlators and on the right we have the Central Mean.

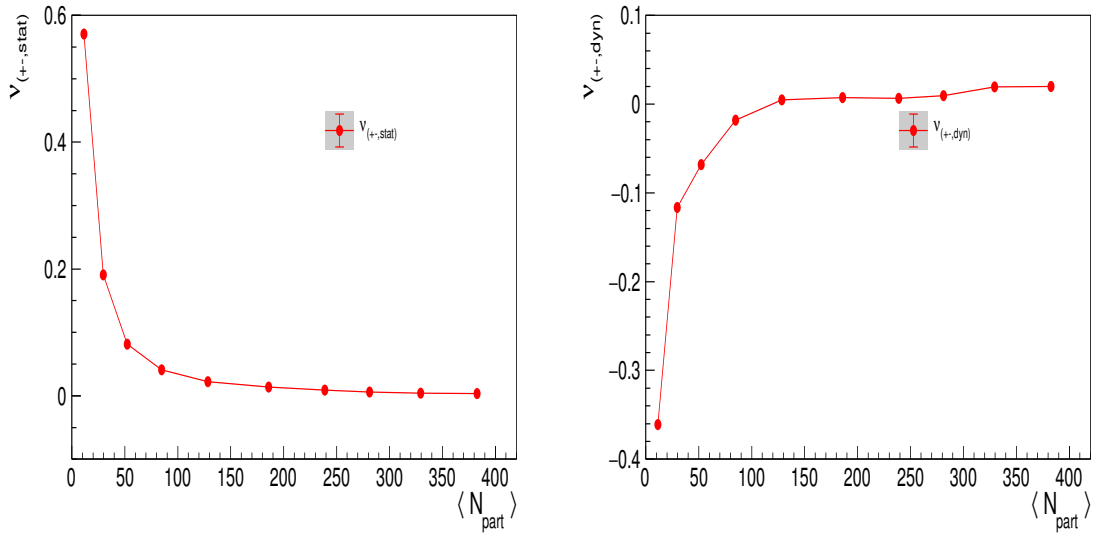

Figure 4.3: On the left we have ν_{stat} and on the right we have $\nu_{dynamics}$.

4.0.2 Poisson

Poisson Fluctuations are calculated to find out how much the actual data is fluctuating from the uncorrelated Poisson values. Poisson distributions describe multiplicities at high energies. Their distribution is :

$$P(X = k) = e^{-\lambda}\frac{\lambda^k}{k!} \tag{4.2}$$

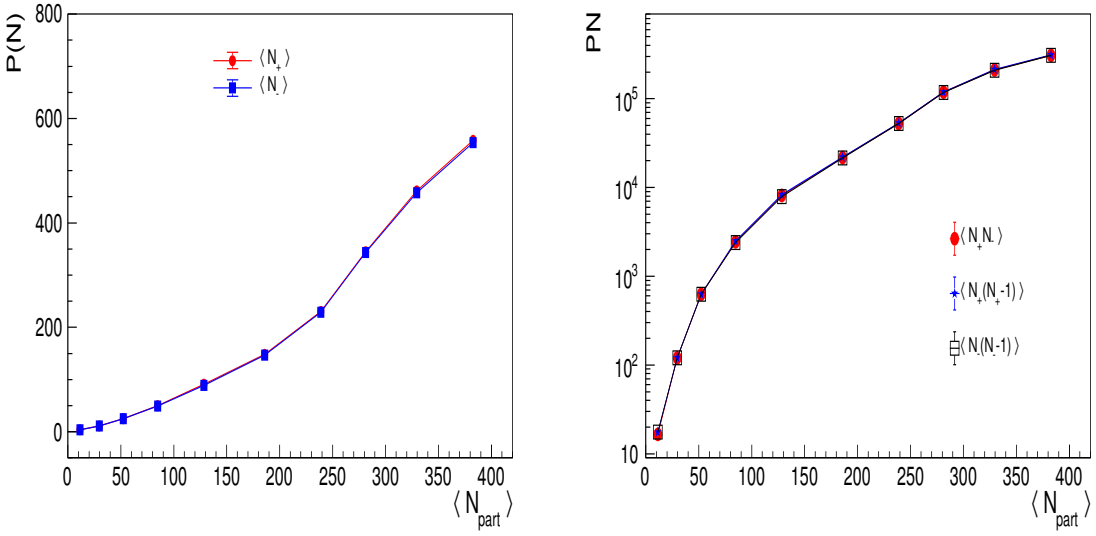

Figure 4.4: On the left we have average values of p and n and on the right we have the factors for choosing two particles if they are same or different.

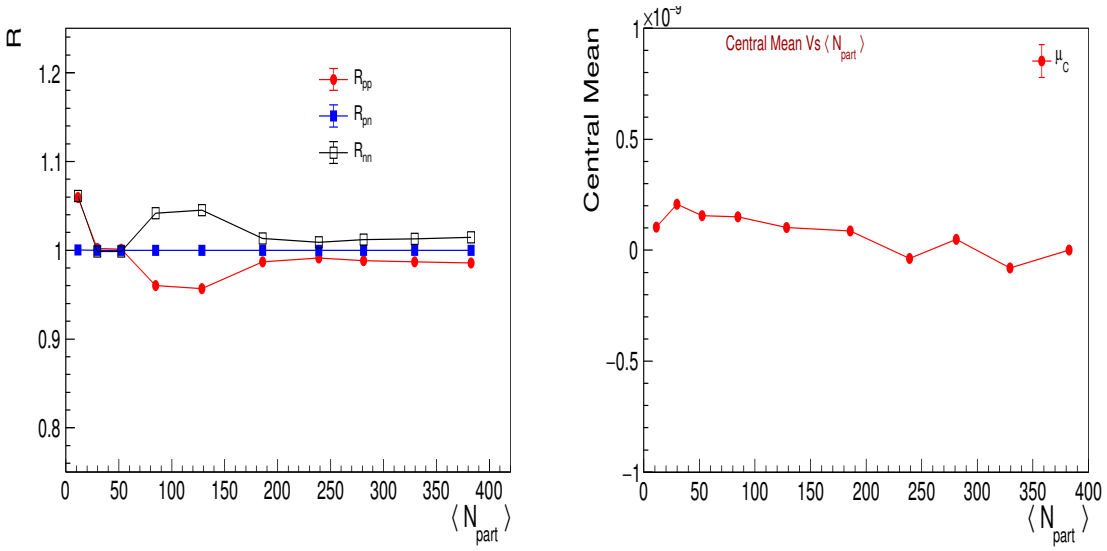

Figure 4.5: On the left we have the particle correlators and on the right we have the Central Mean.

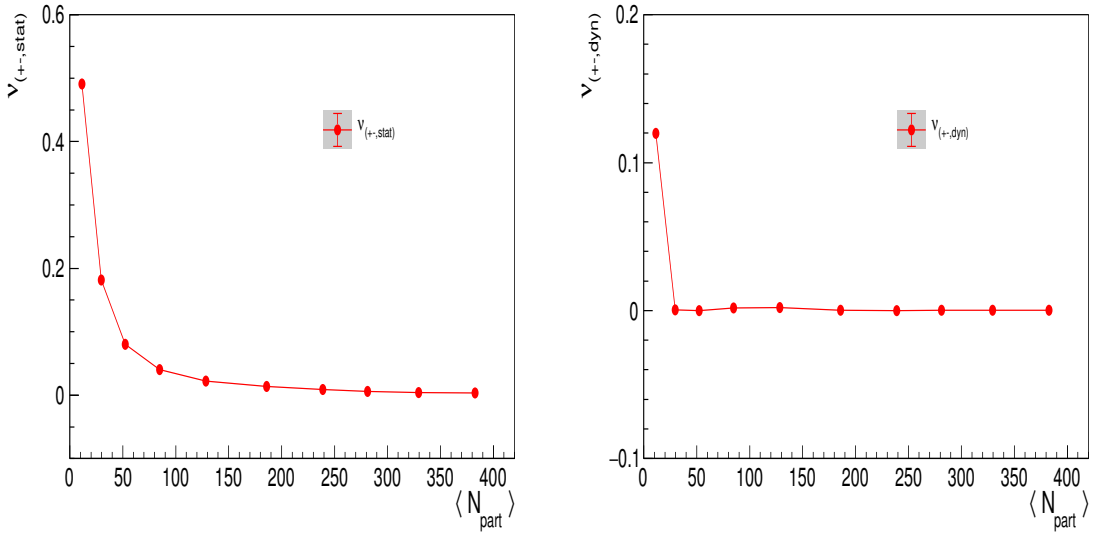

Figure 4.6: On the left we have ν_{stat} and on the right we have $\nu_{dynamics}$. Here we see $\nu_{dynamics}$ tends to 0 since uncorrelated data would mean all its terms become unity.

4.0.3 Physics Model Data (UrQMD)

These plots have been calculated from generated at $\sqrt{S_{NN}}$ = 2.76 TeV in the UrQMD (Ultra Relativistic Quantum Molecular Dynamics) generator. A total of 9.1 Million events have been generated and analysed using the ROOT framework.These are again divided into 4 subsections each for Q - Charge Difference, K - Kaon, π - Pion, p - Proton.

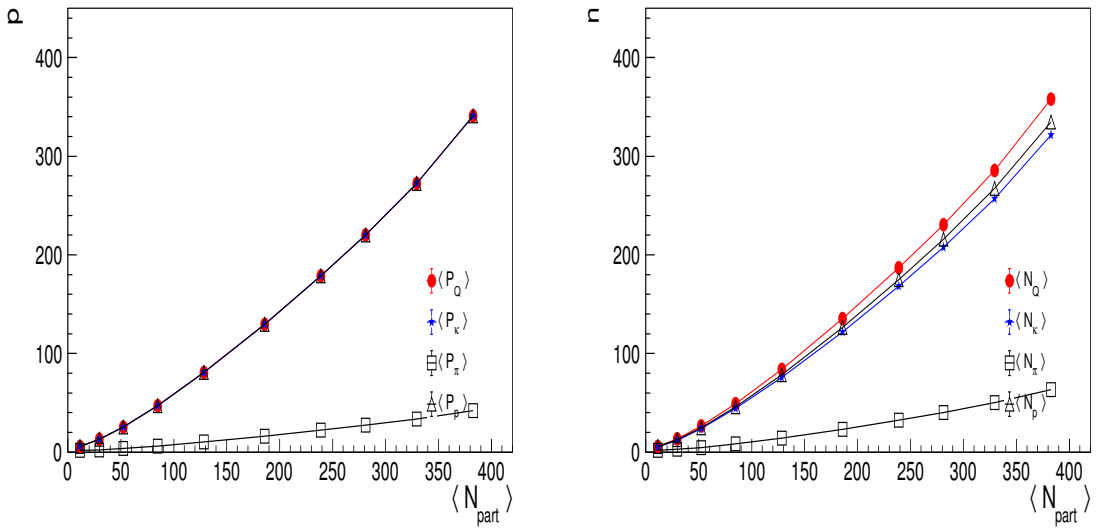

Figure 4.7: On the left we have the average positive values of all different species and its counterpart negative values on the right.

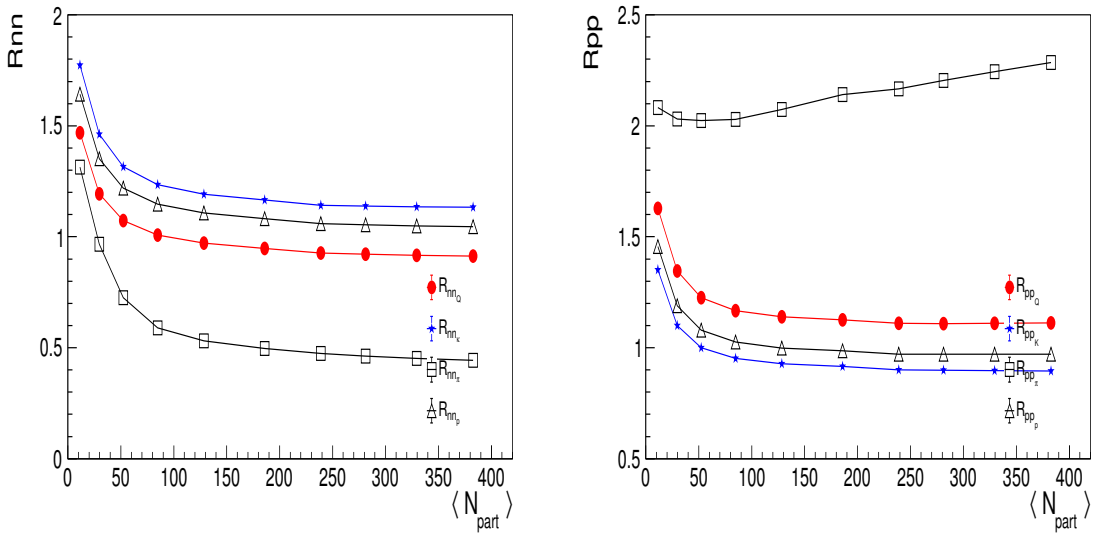

Figure 4.8: On the left we have the negative particle correlator and the positive particle correlator where we see that Pions have high positive particle correlation than its negative particles while rest of the species are more or less uniform.

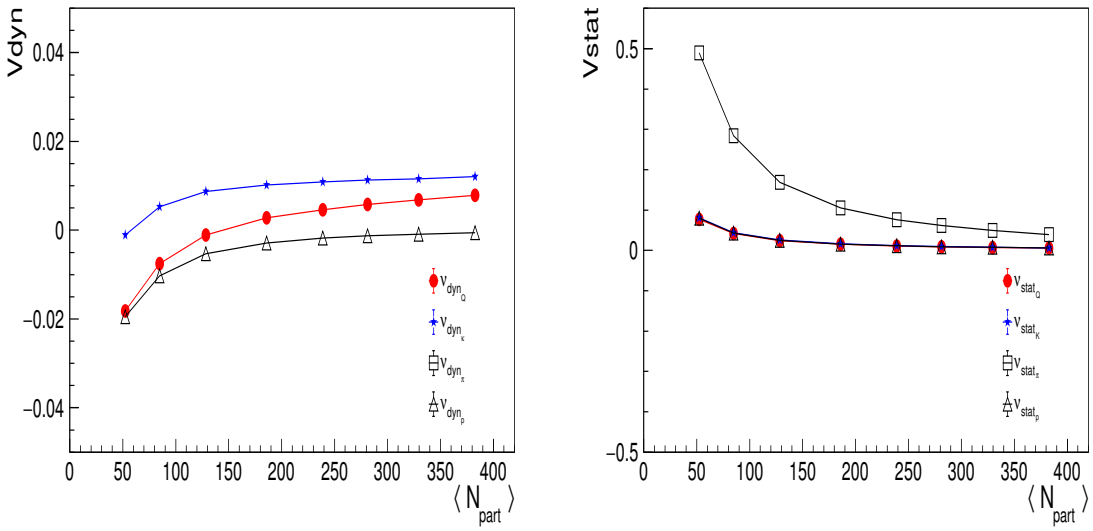

Figure 4.9: On the left we have ν Dynamics and on the right we have ν Stat since the Pion values are shooting up we have zoomed it in the next graph to give some more insight

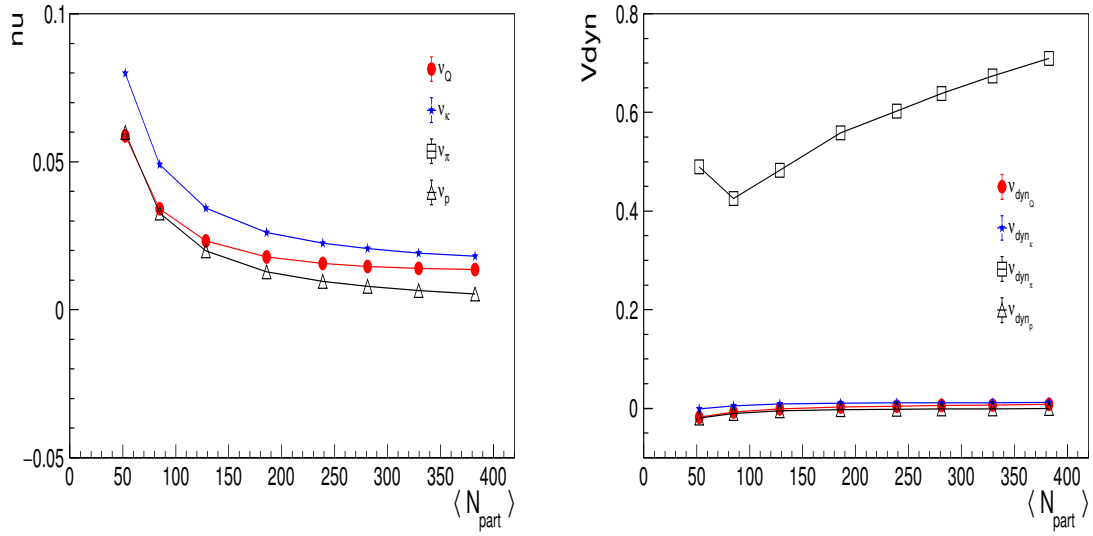

Figure 4.10: On the left we have ν and on the right we have ν dynamics which has been zoomed and it can be seen that with increasing centralities the value is becoming greater implying that at more central collision there is more interaction and equilibriation

Chapter 5

Higher Moment Analysis

The Higher Moment analysis along with expectations from the cases when its purely statistical and uncorrelated particle production and its comparison with experimentally generated data.

5.1 Gaussian Fluctuations

The completely random case is emulated with a normal distribution. 10 Million events were generated for 10 centrality bins with 1 Million in each bin at $\sqrt{s_{NN}}$=2.76 TeV. Gaussian Fluctuation is calculated for accounting for the fluctuations that would come from the statistical fluctuations.

For a variable which has a gaussian distribution its generated by the formula:

$$P(x;\mu;\sigma) = \frac{1}{\sqrt{2\pi}\sigma} e^{\frac{(x-\mu)^2}{2\sigma^2}} \tag{5.1}$$

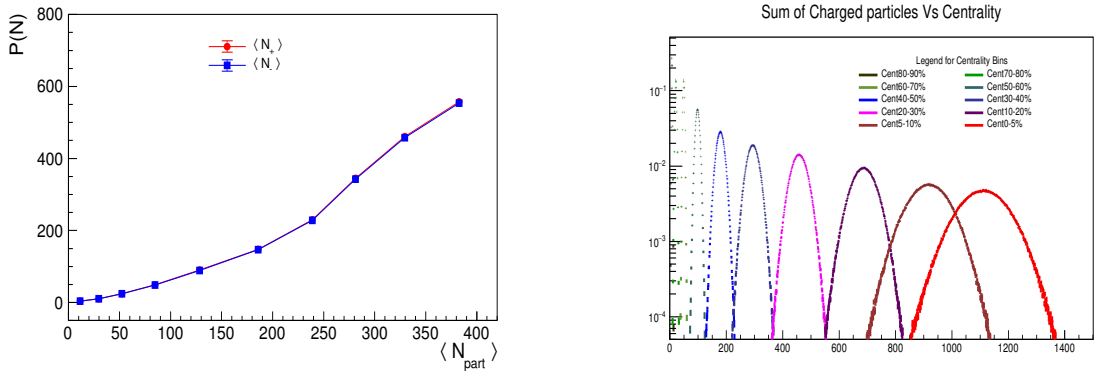

Figure 5.1: On the left we have average p and n values and on the right we have the sum of all charge binned into histograms.

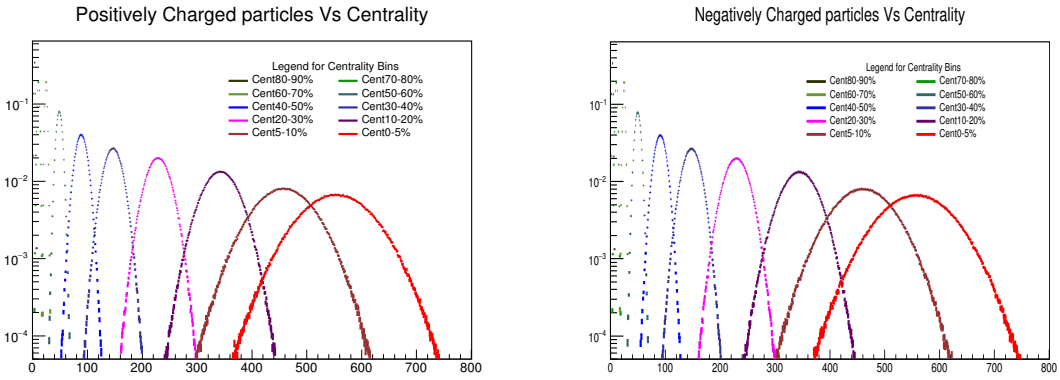

Figure 5.2: On the left we have histogram of positive particles and on the right we have histogram of negative particles

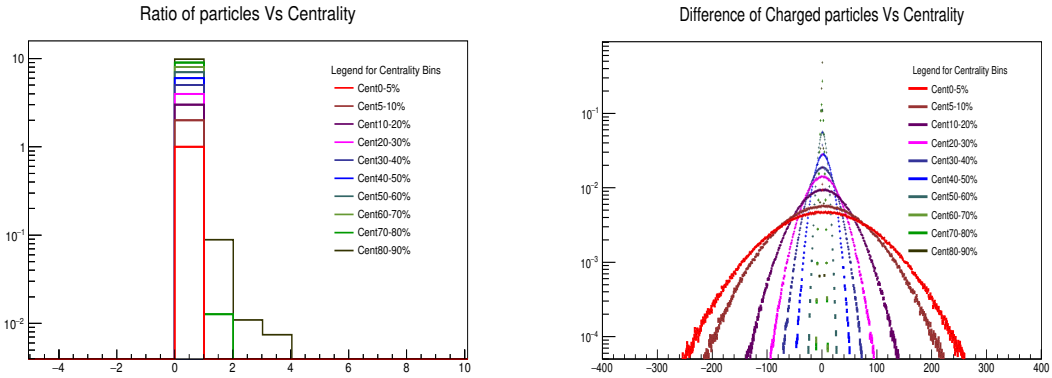

Figure 5.3: On the left we have histogram of Ratios of n/p and on the right the difference n-p histogram

From these distributions the Higher Order Moments were calculated to have an idea how they should look when there is only statistical fluctuations in particle production as opposed to when there would be statistical and dynamical.

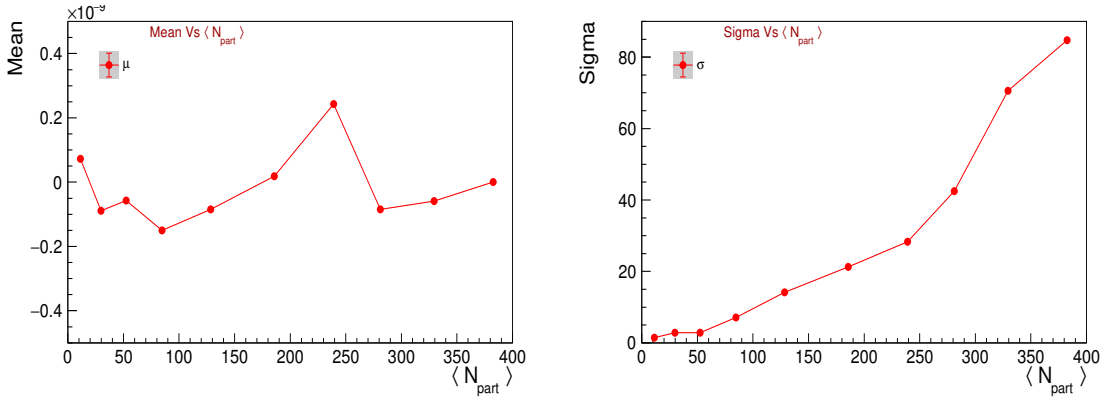

Figure 5.4: On the left we have the mean values and on the right the sigma values

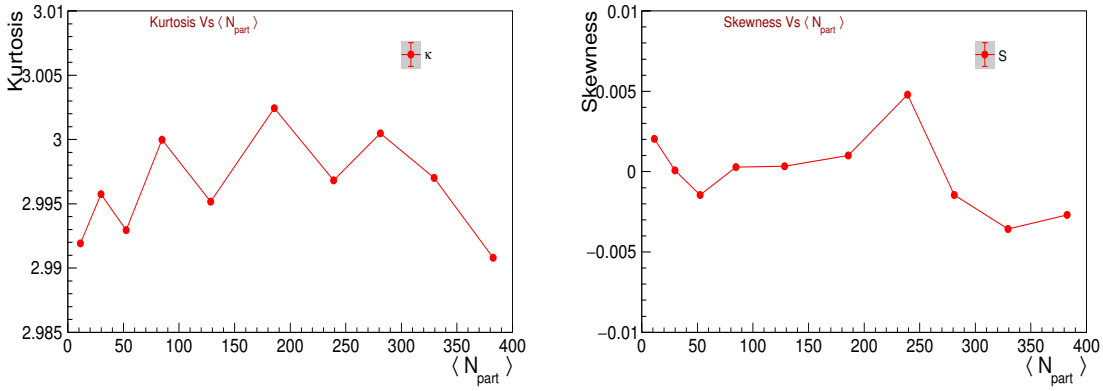

Figure 5.5: On the left we have the Kurtosis and on the right the Skewness, its to be noted that the predicted value of 3.0 for Gaussian is where the Kurtosis is bordering at.

5.2 Poisson Fluctuations

10 Million events were generated for 10 centrality bins with 1 Million in each bin at $\sqrt{s_{NN}}$=2.76 TeV. Negative and Positive particles were generated separately and then charge difference was calculated for which the Higher Order Moments were calculated. The Skellam distribution which was talked about earlier is shown here in the results. Poisson Fluctuations are calculated to find out how much the actual data is fluctuating from the uncorrelated Poisson values. Poisson distributions describe multiplicities at high energies. Their distribution is :

$$P(X = k) = e^{-\lambda}\frac{\lambda^k}{k!} \tag{5.2}$$

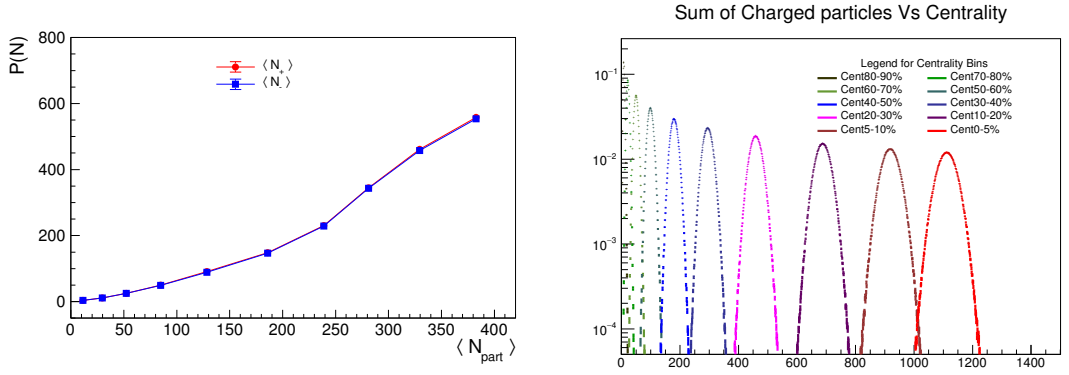

Figure 5.6: On the left we have average p and n values and on the right we have the sum of all charge binned into histograms.

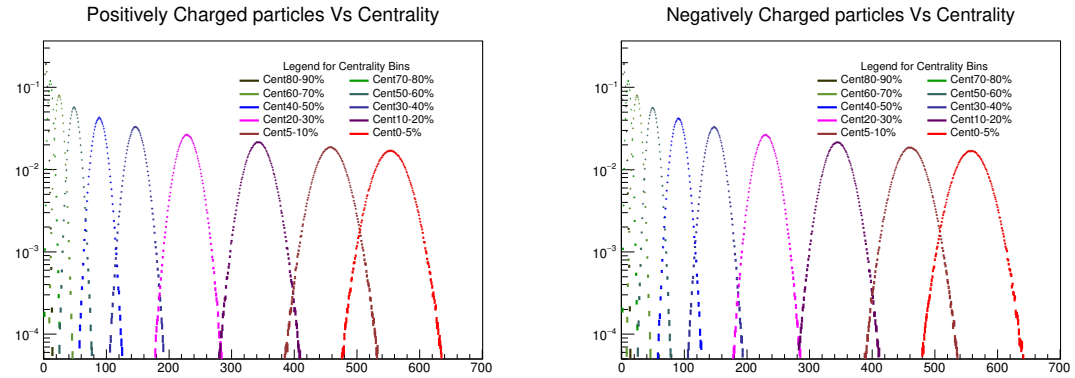

Figure 5.7: On the left we have histogram of positive particles and on the right we have histogram of negative particles

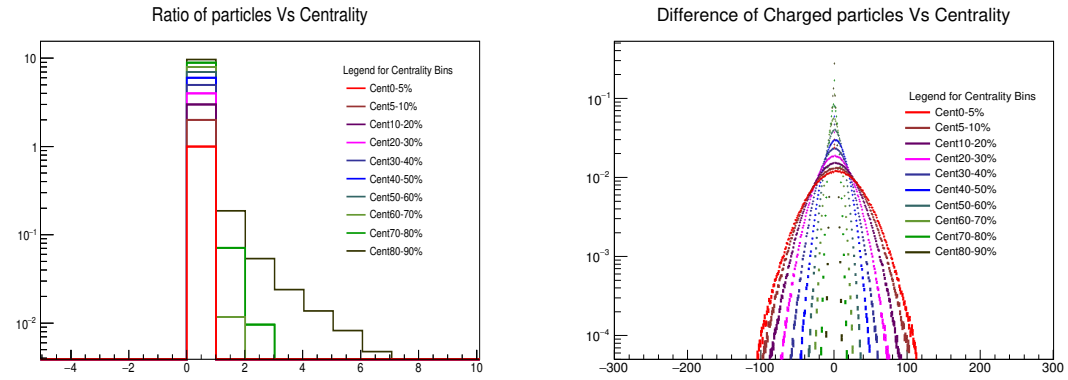

Figure 5.8: On the left we have histogram of Ratios of n/p and on the right the difference n-p histogram

From these distributions the Higher Order Moments were calculated to have an idea how they should look when there is no co-relation in particle production as opposed to when there would be.

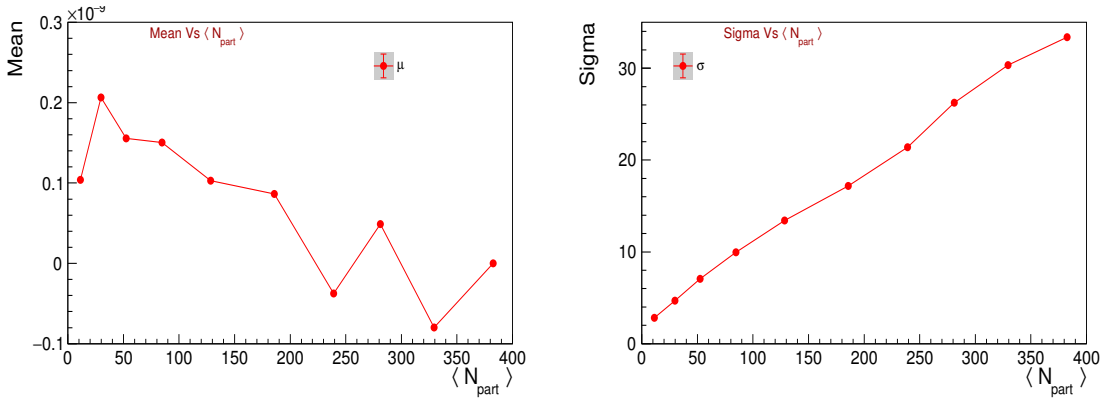

Figure 5.9: On the left we have the mean values and on the right the sigma values

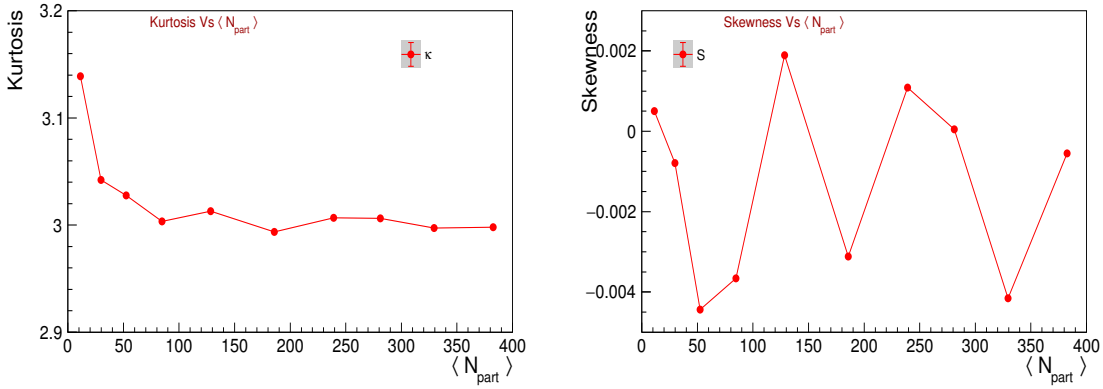

Figure 5.10: On the left we have the Kurtosis and on the right the Skewness, its to be noted that the predicted value of 3.0 for Poisson is where the Kurtosis is bordering at.

5.3 Physics Model Data (UrQMD)

These plots have been calculated from generated at $\sqrt{S_{NN}} = 2.76$ TeV in the UrQMD (Ultra Relativistic Quantum Molecular Dynamics) generator. A total 0f 9.1 Million events have been generated and analysed using the ROOT framework.These are again divided into 4 subsections each for Q - Charge Difference, K - Kaon, π - Pion, p - Proton.

5.3.1 Charge Difference

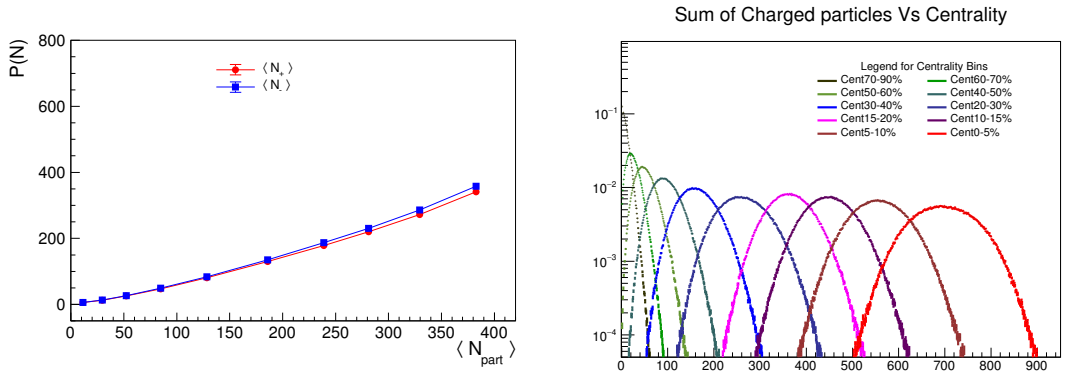

Figure 5.11: On the left we have average n,p values and on the right the total sum of charged particles binned into histograms

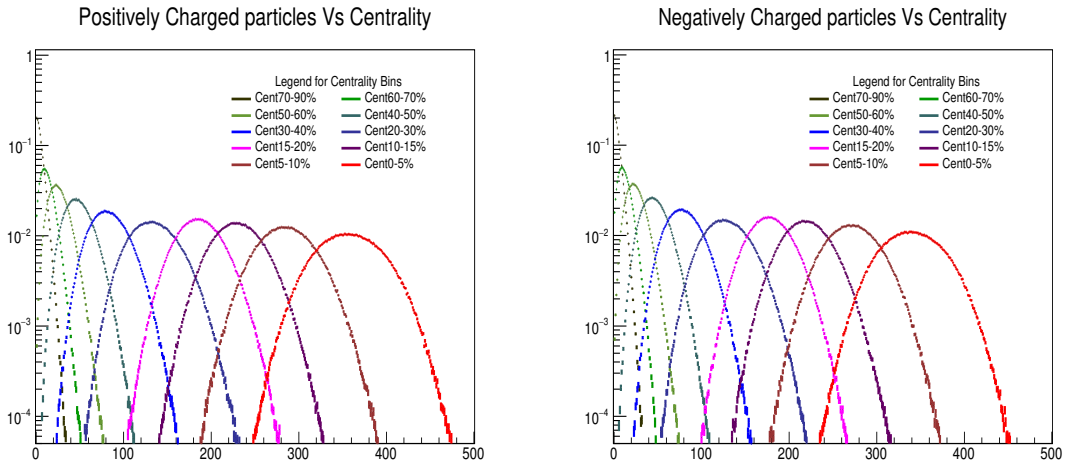

Figure 5.12: On the left we have the histograms of positive particles and on the right the histograms of negative particles

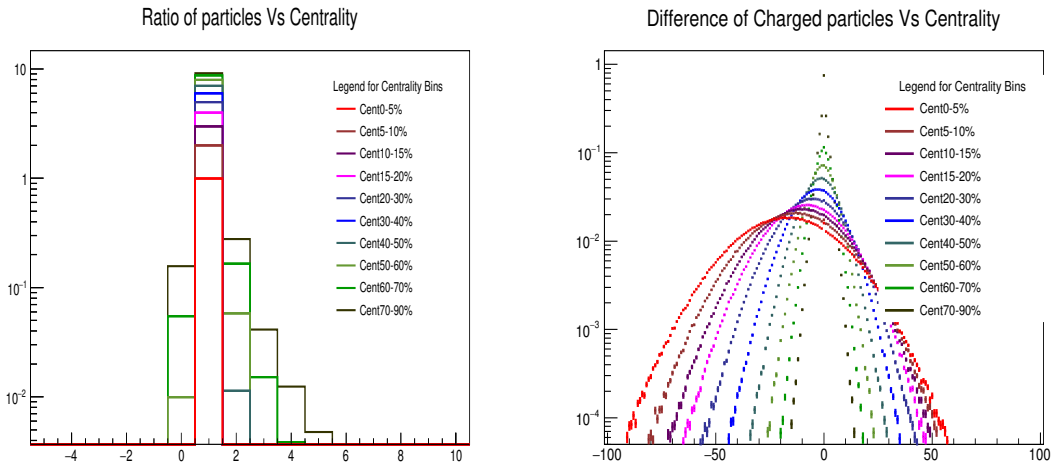

Figure 5.13: On the left we have the ration n/p histograms and on the right the difference n-p histograms

5.4 Kaon, Pion and Proton Particle distributions

The distributions of Kaon, Pion and Proton were also plotted and its statistics have also been calculated. Kaon gives an insight into the Strangeness of the system which was discussed in the earlier sections about Strangeness Enhancement.

Pions make up for the majority of charge contributions to the system.

Protons can tell us about the Baryonic number and also its the only particle that isn't formed through a decay unlike others which have decay sources too.

So studying about these particles can tell us about how these conserved charges are fluctuating in the system.

5.4.1 Kaon

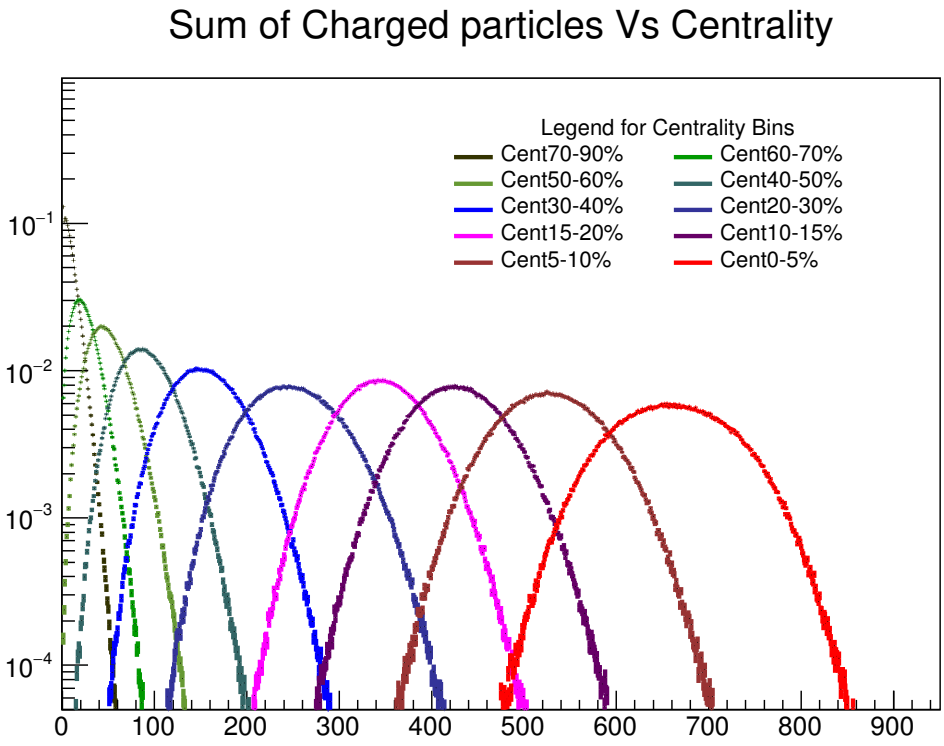

Figure 5.14: Sum of charged particles histograms stacked against centralities

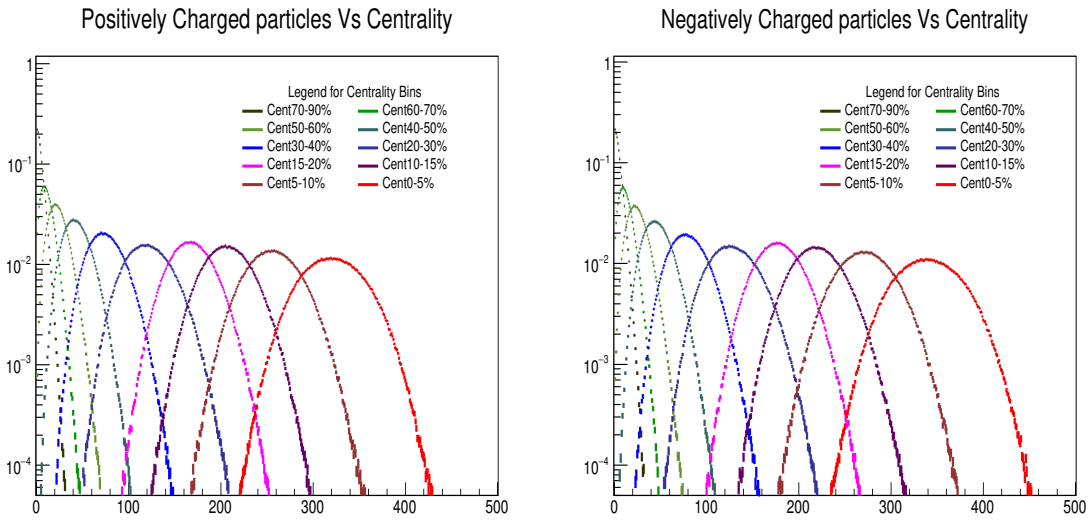

Figure 5.15: On the left we have the histograms of positive particles and on the right the histograms of negative particles

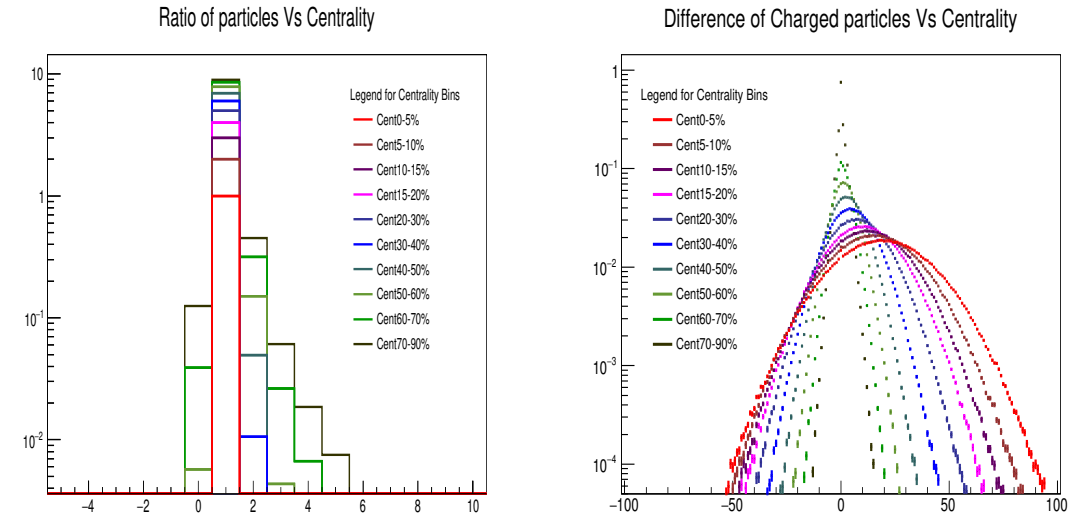

Figure 5.16: On the left we have the ration n/p histograms and on the right the difference n-p histograms

5.4.2 Pion

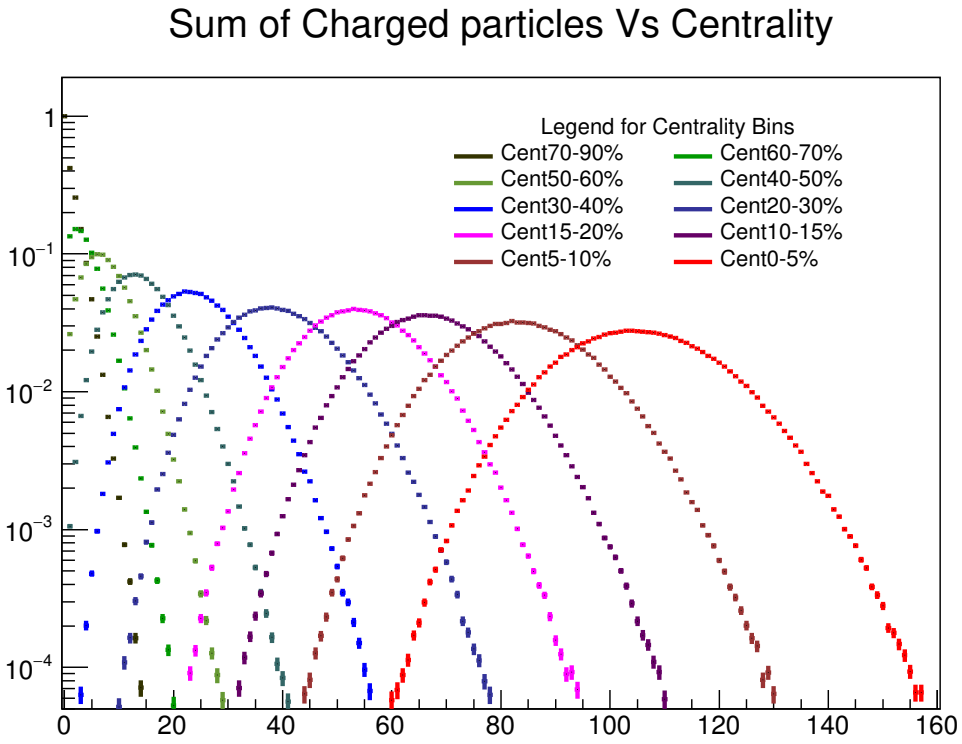

Figure 5.17: Sum of charged particles histograms stacked against centralities

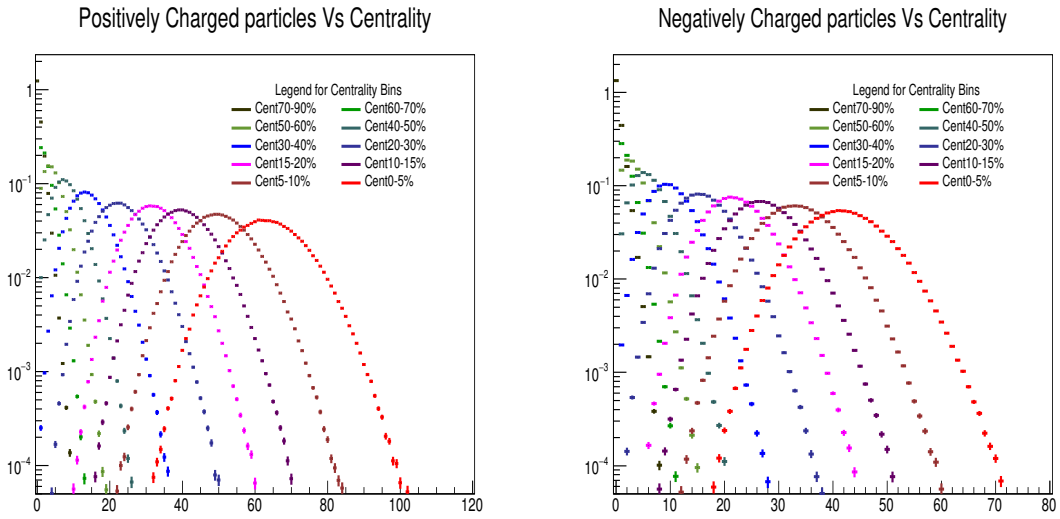

Figure 5.18: On the left we have the histograms of positive particles and on the right the histograms of negative particles

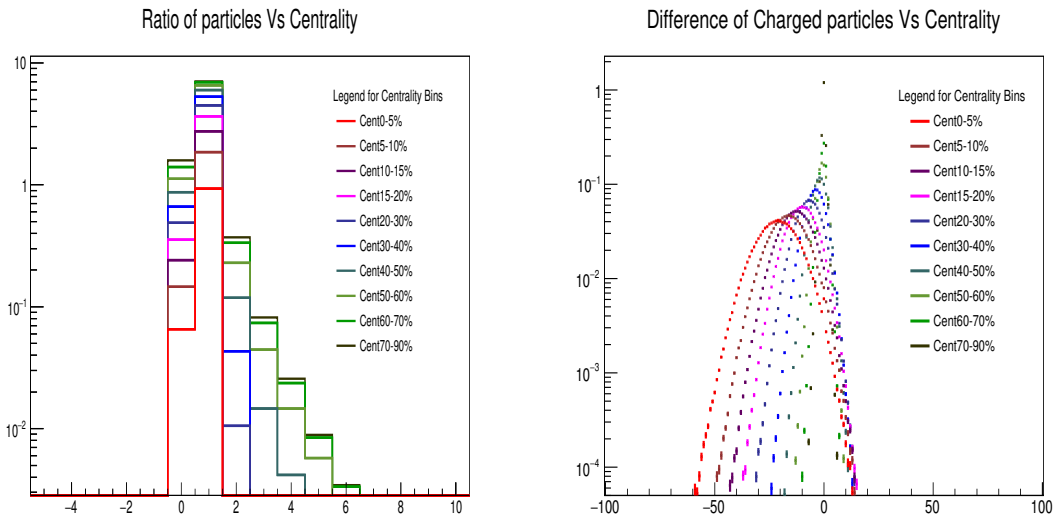

Figure 5.19: On the left we have the ration n/p histograms and on the right the difference n-p histograms

5.4.3 Proton

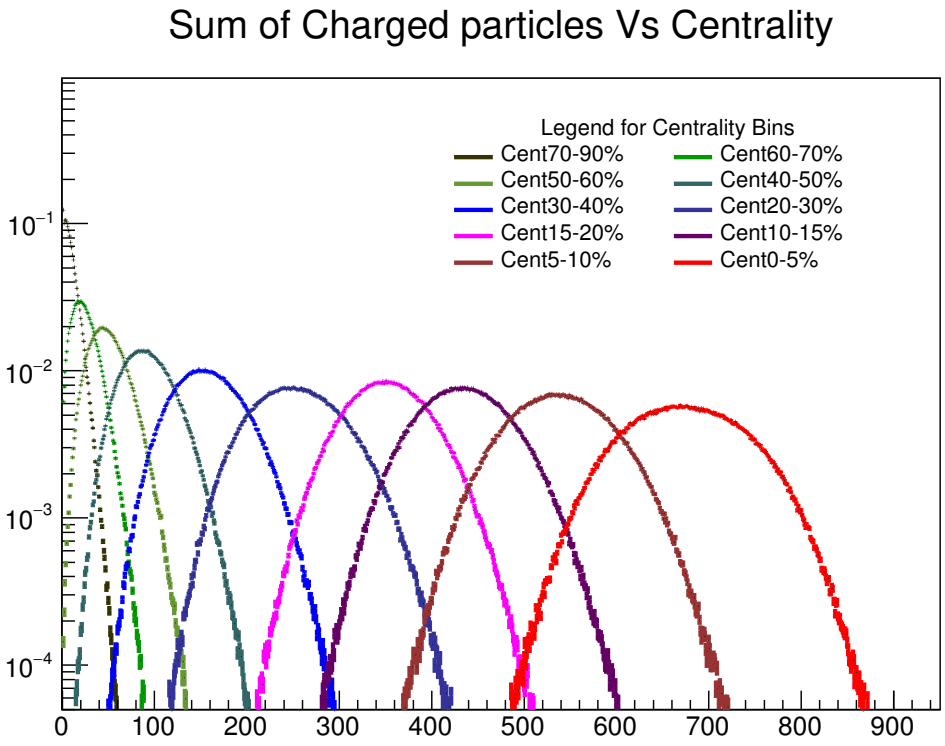

Figure 5.20: Sum of charged particles histograms stacked against centralities

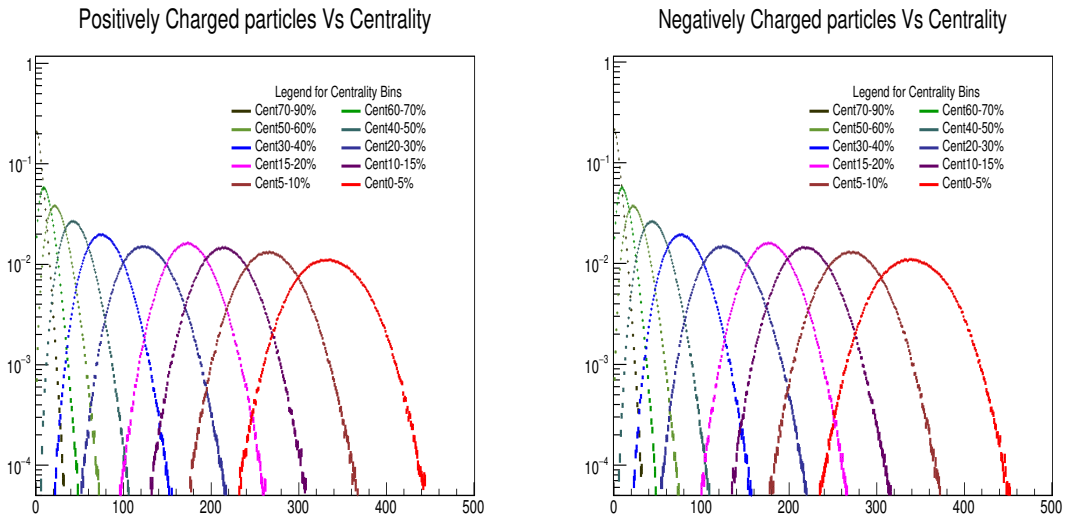

Figure 5.21: On the left we have the histograms of positive particles and on the right the histograms of negative particles

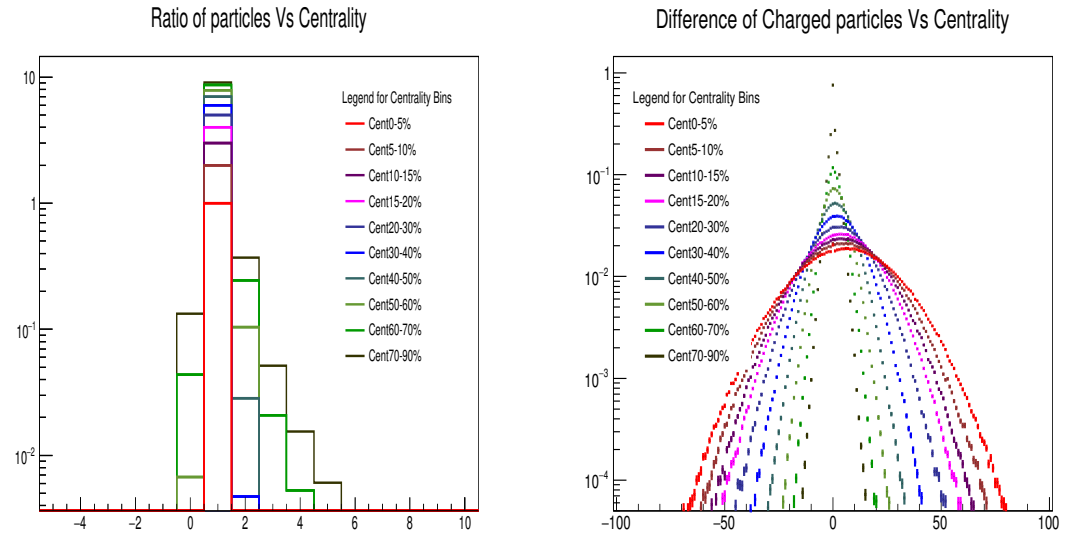

Figure 5.22: On the left we have the ration n/p histograms and on the right the difference n-p histograms

From these distributions 10 quantities were calculated for probing the system for better viewing purposes all the different particle species have been plotted together.

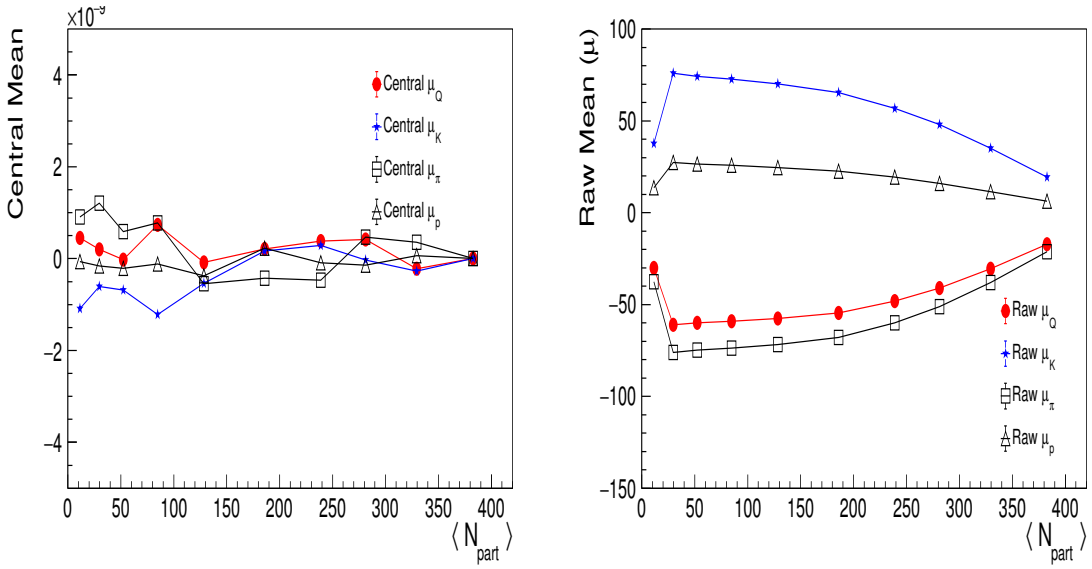

Figure 5.23: On the left we have Central mean for different species and on the right the Raw mean

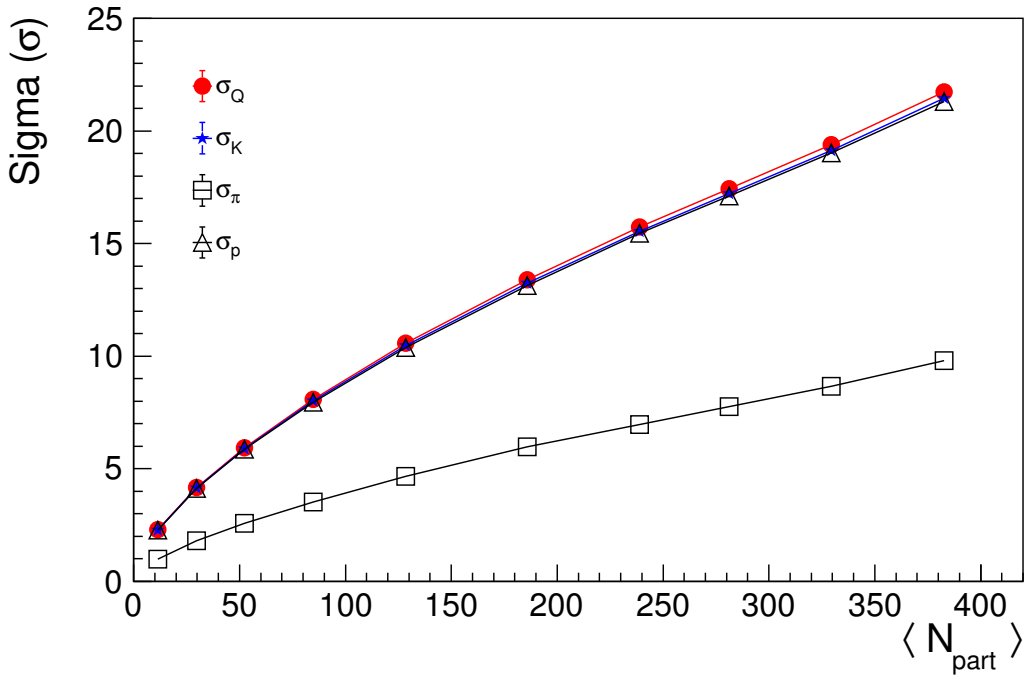

Figure 5.24: The plot of sigma values for different species

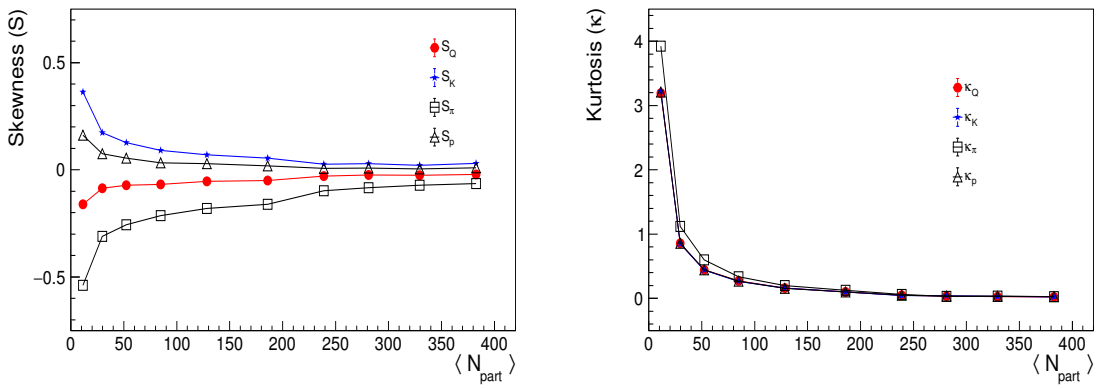

Figure 5.25: On the left we have Skewness and on the right we have Kurtosis both for various species

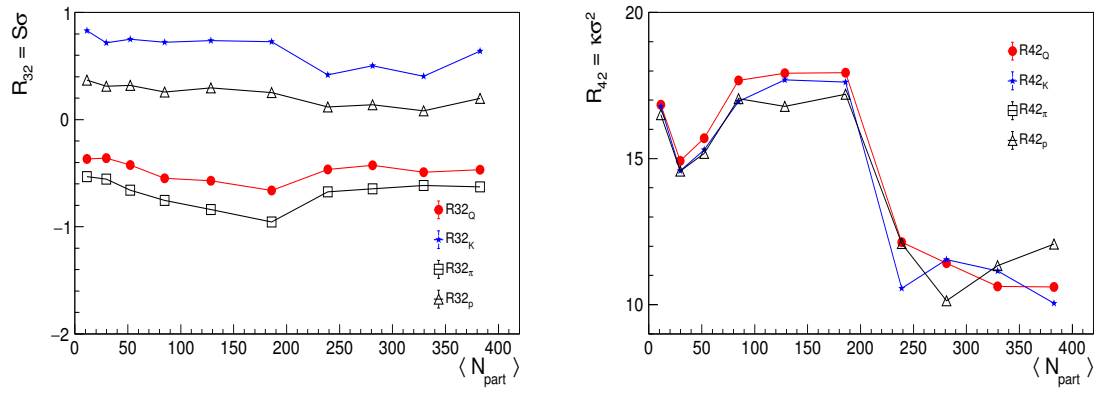

Figure 5.26: On the left we have susceptibilities R_{32} and on the right R_{42}.

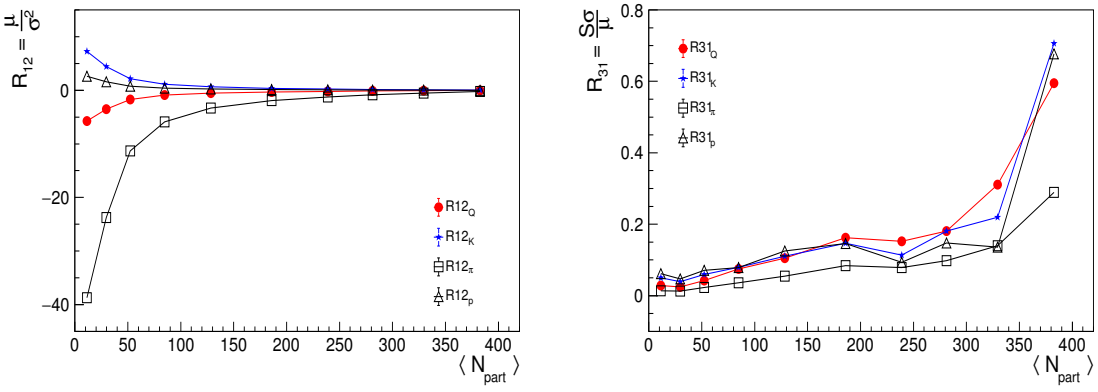

Figure 5.27: On the left we have susceptibilities R_{12} and on the right R_{31}

The last 4 quantities are called co-relators which tell us about the susceptibilities of the system when undergoing fluctuations. Conserved quantities will give us an opportunity to study about the system in a different way. Their fluctuations over system can give important

results on the parameters which we are looking for. The susceptibility of the system plays an important role here. Susceptibility, χ, of a system tells us the response of that system to some perturbation.

They can be found out from the central moments.

$$R_{32} = S\sigma$$
$$R_{42} = \kappa\sigma^2$$
$$R_{12} = \frac{\mu}{\sigma^2}$$
$$R_{31} = \frac{S\sigma^2}{\mu}$$

All of these cumulants or central moments have been calculated for the quantity N = $Q - < Q >$, where Q = n-p.

n is the number of negatively charged particles and p is the number of positively charged particles. We know that cumulants of N in a statistical system are extensive variables [AK16].

The generalised susceptibility of conserved quantities are obtained by taking the derivative of dimensionless pressure as,

$$\chi^{BSQ}_{lmn} = \frac{\partial^{l+m+n}(\frac{P}{T^4})}{\partial(\frac{\mu_B}{T})^l \partial(\frac{\mu_S}{T})^m \partial(\frac{\mu_Q}{T})^n} \tag{5.3}$$

where B, S, Q are the conserved quantities of QCD, and l, m, n denotes the higher order derivatives. This susceptibility is also related to the moments of the distribution. For large number of events higher order moments can be calculated and it will give a good understanding about the QCD observables.

Here are the the relation between susceptibility and higher moments (up to fourth moment),

$$\mu = VT^3\chi_1 \tag{5.4}$$
$$\sigma^2 = VT^3\chi_2 \tag{5.5}$$
$$S = VT^3\chi_3 \tag{5.6}$$
$$\kappa = VT^3\chi_4 \tag{5.7}$$

These ratios become exactly unity in the HRG model. These ratios thus are suitable in exploring the existence of physics which cannot be described by the HRG model [AK16].

Chapter 6

Summary

In this work we mainly focused on the study of fluctuations in heavy ion collisions at $\sqrt{S_{NN}}$ =2.76 TeV. Here we are briefly collating all the results and important conclusions. From statistical mechanics, we got the idea to treat the system formed during collision as an ensemble, and from there the possibilities of calculating higher moments arose. After calculating the higher order moments we connected the moments of the system to the susceptibility of QCD, which is related to the macroscopic parameters of QGP system. From the susceptibilities there is a deviation from unity which implies fluctuations due to QGP formation.The analysis of Kurtosis (κ) and Skewness (S) have shown there is a charge conservation fluctuation happening, which is a measure of dynamical changes happening inside the system, and thus the study of higher moments is relevant.

We collected data for the collision at 2.76 T eV for three different particles, pions, kaons, proton and anti proton from the transverse momentum distribution. From that data, with the help of a data analysis frame work called ROOT, we were able to calculate the statistics for random fluctuations. Using which we compared it to the statistics for the generated data events.

Other dynamic observables like ν Dynamics, ν Statistics and ν were also calculated to study the dynamical fluctuations better.

Appendix A

Classical Ideal gas in a Grand Canonical Ensemble

The single particle partition function for a classical ideal gas in three dimensions is by

$$Z = \frac{1}{(2\pi\hbar)^3} \int d^3q \int d^3p e^{-\beta H} \tag{A.1}$$

where (q,p) are the coordinates of the particle in phase space. The hamiltonian H is by

$$H = \sum_i \frac{p_i^2}{2m} \tag{A.2}$$

$$Z = \frac{1}{(2\pi\hbar)^3} \int d^3q \int d^3p e^{-\beta p^2/2m} \tag{A.3}$$

$$Z = \frac{1}{(2\pi\hbar)^3} \int d^3q \int d^3p e^{-\beta p^2/2m} = \frac{V}{(2\pi\hbar)^3} \int_0^{\inf} 4\pi p^2 e^{-\beta p^2/2m} dp \tag{A.4}$$

Solving this integral and simplifying the expression, we get

$$Z = V \left(\frac{m k_B T}{2\pi\hbar^2} \right)^{3/2} \tag{A.5}$$

The N particle partition function is

$$q = \frac{1}{N!} Z^N \tag{A.6}$$

The factor of 1/N! accounts for the indistinguishability of the particles. The corresponding grand canonical partition function is defined as

$$Q = \sum_N e^{\beta \mu N} q \tag{A.7}$$

where μ is the chemical potential of the system.

$$Q = \sum_N e^{\beta\mu N} \frac{1}{N!} Z^N \tag{A.8}$$

This can be further simplified as

$$Q = \sum_N e^{\beta\mu N} \frac{1}{N!} Z^N = exp(Ze^{\beta\mu}) \tag{A.9}$$

Once we have the partition function, we can define the average number of particles as

$$< N >= \frac{1}{\beta Q} \frac{\partial Q}{\partial \mu} = \frac{1}{\beta Q} (Q\beta Z e^{\beta\mu}) = Ze^{\beta\mu} \tag{A.10}$$

Now, using the above equation

$$< N^2 > - < N >^2 = k_B T (\frac{\partial < N >}{\partial \mu}) = Ze^{\beta\mu} =< N > \tag{A.11}$$

Bibliography

[AAA+03] D Adamova, G Agakichiev, H Appelshäuser, V Belaga, P Braun-Munzinger, A Cherlin, S Damjanović, T Dietel, L Dietrich, A Drees, et al., *Enhanced production of low-mass electron-positron pairs in 40-a gev pb-au collisions at the cern sps*, Physical review letters **91** (2003), no. 4, 042301.

[ABB+04] T. Anticic, B. Baatar, D. Barna, J. Bartke, M. Behler, L. Betev, H. Bialkowska, A. Billmeier, C. Blume, B. Boimska, M. Botje, J. Bracinik, R. Bramm, R. Brun, P. Bunčić, V. Cerny, P. Christakoglou, O. Chvala, J. G. Cramer, P. Csató, N. Darmenov, A. Dimitrov, P. Dinkelaker, V. Eckardt, P. Filip, D. Flierl, Z. Fodor, P. Foka, P. Freund, V. Friese, J. Gál, M. Gaździcki, G. Georgopoulos, E. Gładysz, K. Grebieszkow, S. Hegyi, C. Höhne, K. Kadija, A. Karev, V. I. Kolesnikov, T. Kollegger, R. Korus, M. Kowalski, I. Kraus, M. Kreps, M. van Leeuwen, P. Lévai, L. Litov, M. Makariev, A. I. Malakhov, C. Markert, M. Mateev, B. W. Mayes, G. L. Melkumov, C. Meurer, A. Mischke, M. Mitrovski, J. Molnár, St. Mrówczyński, G. Pálla, A. D. Panagiotou, D. Panayotov, A. Petridis, M. Pikna, L. Pinsky, F. Pühlhofer, J. G. Reid, R. Renfordt, W. Retyk, C. Roland, G. Roland, M. Rybczyński, A. Rybicki, A. Sandoval, H. Sann, N. Schmitz, P. Seyboth, F. Siklér, B. Sitar, E. Skrzypczak, G. Stefanek, R. Stock, H. Ströbele, T. Susa, I. Szentpétery, J. Sziklai, T. A. Trainor, D. Varga, M. Vassiliou, G. I. Veres, G. Vesztergombi, D. Vranić, A. Wetzler, Z. Włodarczyk, I. K. Yoo, J. Zaranek, and J. Zimányi, *Transverse momentum fluctuations in nuclear collisions at* $158a\ \mathrm{GeV}$, Phys. Rev. C **70** (2004), 034902.

[AK16] Masayuki Asakawa and Masakiyo Kitazawa, *Fluctuations of conserved charges in relativistic heavy ion collisions: An introduction*, Progress in Parti-

cle and Nuclear Physics **90** (2016), 299–342.

[Alf03] M Alford, *Qcd at high density/temperature*, Nuclear Physics B-Proceedings Supplements **117** (2003), 65–82.

[and08] S M Dogra and, *Star measurements of correlations and fluctuations between photons and charged particles at forward rapidities at rhic*, Journal of Physics G: Nuclear and Particle Physics **35** (2008), no. 10, 104094.

[C+12] ALICE Collaboration et al., *Net-charge fluctuations in pb-pb collisions at* $\sqrt{s_{NN}} = 2.76tev$, arXiv preprint arXiv:1207.6068 (2012).

[Cha14] A. K. Chaudhuri, *A short course on Relativistic Heavy Ion Collisions*, IOPP, 2014.

[DC+07] S Damjanovic, NA60 Collaboration, et al., *Na60 results on the ρ spectral function in in-in collisions*, Nuclear Physics A **783** (2007), no. 1-4, 327–334.

[GG11] RV Gavai and Sourendu Gupta, *Lattice qcd predictions for shapes of event distributions along the freezeout curve in heavy-ion collisions*, Physics Letters B **696** (2011), no. 5, 459–463.

[GM92] Marek Gaździcki and Stanisław Mrówczyński, *A method to study ?equilibration? in nucleus-nucleus collisions*, Zeitschrift für Physik C Particles and Fields **54** (1992), no. 1, 127–132.

[GO09] Jan Fiete Grosse-Oetringhaus, *Measurement of the Charged-Particle Multiplicity in Proton-Proton Collisions with the ALICE Detector*, Ph.D. thesis, Muenster, Germany, University of Muenster, Germany, 2009.

[GP90] Miklos Gyulassy and Michael Plumer, *Jet quenching in dense matter*.

[Hal00] Anders Hald, *The early history of the cumulants and the gram-charlier series*, International Statistical Review **68** (2000), no. 2, 137–153.

[KH04] Peter F Kolb and Ulrich Heinz, *Hydrodynamic description of ultrarelativistic heavy-ion collisions*, Quark–Gluon Plasma 3, World Scientific, 2004, pp. 634–714.

[KR11] Frithjof Karsch and Krzysztof Redlich, *Probing freeze-out conditions in heavy ion collisions with moments of charge fluctuations*, Physics Letters B **695** (2011), no. 1-4, 136–142.

[Luo11] Xiaofeng Luo, *Higher Moments of Event-by-Event Net-proton Multiplicity Distributions in Ultra-relativistic Heavy Ion Collision*, Ph.D. thesis, Hefei, CUST, 2011.

[MRSS07] Michael L Miller, Klaus Reygers, Stephen J Sanders, and Peter Steinberg, *Glauber modeling in high-energy nuclear collisions*, Annu. Rev. Nucl. Part. Sci. **57** (2007), 205–243.

[PGV02] C. Pruneau, S. Gavin, and S. Voloshin, *Methods for the study of particle production fluctuations*, Phys. Rev. C **66** (2002), 044904.

[Pis82] Robert D Pisarski, *Phenomenology of the chiral phase transition*, Physics Letters B **110** (1982), no. 2, 155–158.

[PP00] Stefan Pokorski and Stefan Pokorski, *Gauge field theories*, vol. 92, Cambridge University Press Cambridge, 2000.

[Sat06] Helmut Satz, *Colour deconfinement and quarkonium binding*, Journal of Physics G: Nuclear and Particle Physics **32** (2006), no. 3, R25.

[ST09] Thomas Schäfer and Derek Teaney, *Nearly perfect fluidity: from cold atomic gases to hot quark gluon plasmas*, Reports on Progress in Physics **72** (2009), no. 12, 126001.

[Tra00] TA Trainor, *Event-by-event analysis and the central limit theorem*, arXiv preprint hep-ph/0001148 (2000).

[TW02] Boris Tomasik and Urs Wiedemann, *Central and non-central hbt from ags to rhic*.